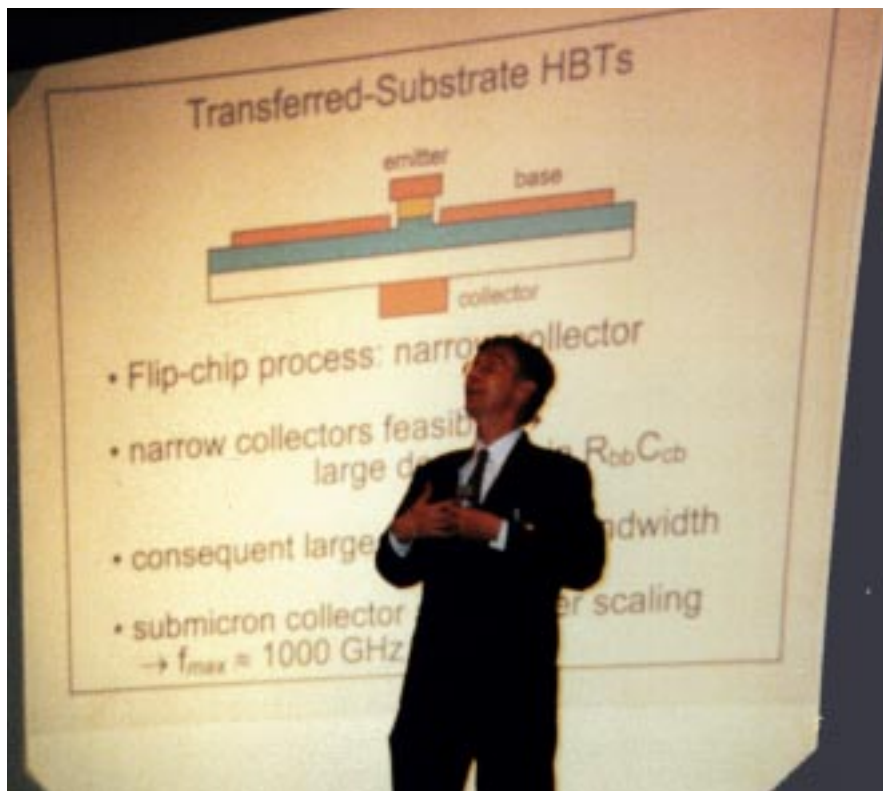

MICROELECTRONICS AND OPTOELECTRONICS LABORATORY

Indium Phosphide and Related Materials (IPRM'99)



May 16 - 20, 1999
Congress Center Davos
Davos, Switzerland



Previous Page:

Indium Phosphide and Related Materials Conference (IPRM'99) in Davos with Marc Rodwell, Prof. at the University of California, Santa Barbara, U.S.A. presenting his landmark Terahertz Transistors made from Indium Phosphide.

CONTENTS

PERSONNEL

RESEARCH SUMMARY

Educational Activities

General Activities

MICRO- AND OPTOELECTRONICS LABORATORY

Low Pressure Metal Organic Vapor Phase Epitaxy for Three-Five Compound Semiconductors

Plasma Etching

All-Optical-Switches in Mach-Zehnder Configuration for Optical Communication Systems

All-Optical Switches with Monolithically Integrated Phase Shifters

All-Optical Mach-Zehnder Interferometer Modeling

Nonlinear Dynamics Simulations and Measurements in Semiconductor Optical Amplifiers

Novel Concept for All-Optical Add/Drop Multiplexing with Regenerative Capability

Optical Data Regeneration at 40 Gbit/s

Ultra-fast All-Optical Demultiplexer for 160 Gbit/s Networks

All-Optical Wavelength Conversion at 10 Gbit/s over Extended 80 nm Wavelength Range

Mode-Locked Laser Diodes with External Fiber Bragg Grating Cavity

Saturable Absorbers Realized by Heavy Ion Implantation for Mode-Locked Semiconductor Laser Diodes

Wavelength-Tunable Pulse Source at 5-40 GHz by Optical Modulation of a Semiconductor Optical Amplifier in a Fibre Ring Laser

Chirp Dynamics in Wavelength Conversion using Semiconductor Optical Amplifiers

Active Multi-Mode-Interferometer Semiconductor Optical Amplifier

Analysis of Electro-Optic Effects in InP / InGaAsP Based Waveguide Structures

High Output Powers from Semiconductor Laser Diode Arrays Coherently Coupled in Mach-Zehnder Configuration

Silica-on-Silicon Multi-Channel Phased Array Wavelength Filters

Spectrally Sliced Amplified Spontaneous Emission Source

Polarization Insensitive Arrayed Waveguide Grating Filters in Indium Phosphide Applying Birefringence Compensation Scheme

Monolithic InGaAs/InP pin/HBT Optical Receiver Front-End Module for Data Rates up to 40 Gb/s

High-Current Indium Phosphide Double Heterostructure Bipolar Transistor Driver Circuits for Laser Diodes

Fiber Optical Burst-Mode Packet Receivers Operating at 155 Mbit/s and 622 Mbit/s

Complimentary Metal-Oxide Semiconductor Electronics for Processor to Processor Optical Interconnects

CMOS Laser Drivers for 4 Gbit/s Optical Interconnects

Large Area Solar-blind PtSi-nSi Photodetectors

New Insights into Low Dimensional Structures and Wafer Fused Devices

Opto Speed SA

THIN FILM PHYSICS GROUP

Development of Superstrate $\text{Cu}(\text{In},\text{Ga})\text{Se}_2$ Solar Cells

Lightweight and Flexible $\text{Cu}(\text{In},\text{Ga})\text{Se}_2$ Solar Cells on Polymer with a World Record Efficiency of 12.8%

CdTe/CdS Thin Film Solar Cells

Efficient and Stable Electrical Contacts on CdTe/CdS Solar Cells

Heteroepitaxial High Quality Narrow Gap Lead-Chalcogenides on Si(111) and Formation of Quantum Dots

Development Steps of a 128 x 96 Heteroepitaxial Narrow Gap Infrared Sensor Array on a Silicon Read-Out Chip

Packaging of PbTe-on-Si Infrared Sensor Arrays for Thermal Imaging

PUBLICATIONS 1999

Micro- and Optoelectronics Laboratory

Thin Film Physics Group at Institute of Quantum Electronics

ORAL PRESENTATIONS 1999

PERSONNEL

Microelectronics and Optoelectronics Laboratory

Head

Melchior, Hans, Prof. Dr.

Academic and Corporate Guests

Kneubühl, Fritz K., Prof. Dr.

Hamamoto, Kiichi, NEC Corporation, Ibaraki, Japan

Kawaguchi, Hitoshi, Prof., Yamagata University, Japan

Kawazoe, Tadashi, Dr., Yamagata University, Japan

Soto Ortiz, Horacio, Dr., CICESE, Ensenada, Mexico

Skovgaard, Peter M.W., Dr., DTU Lyngby, Danmark

Dall'Ara, Roberto, Opto Speed SA, Mezzovico, Switzerland

Blaser, Markus, Dr., Opto Speed SA, Mezzovico, Switzerland

Blaser, Hanspeter, Opto Speed SA, Mezzovico, Switzerland

Bauknecht, Raymond, Dr., Opto Speed SA, Mezzovico, Switzerland

Eckner, Jürg, Dr., Opto Speed SA, Mezzovico, Switzerland

Holtmann, Christoph, Dr., Opto Speed SA, Mezzovico, Switzerland

Hunziker, Werner, Dr., Opto Speed SA, Mezzovico, Switzerland

Leibinger Fasler, Maria, Opto Speed SA, Mezzovico, Switzerland

Rezzonico, Raffaele, Opto Speed SA, Mezzovico, Switzerland

Wieland, Jörg, Dr., Helix AG, Zurich, Switzerland

Team Leaders

Guekos, Georg, Dr., Associate Professor

Academic Staff

Annen, Richard, Dipl. El.-Ing. ETH

Bitter, Martin, Dipl. El.-Ing. ETH

Bossard, Martin, Dipl. El.-Ing. ETH

Caraccia-Gross, Muriel, Dipl. Phys. ETH

Dülk, Marcus, Dipl. Phys. TU Berlin

Fischer, Stefan, Dipl. Phys. ETH

Gamper, Emil, Dipl. Phys. ETH

Gini, Emilio, Dr. sc.nat. ETH

Hagn, Gerhard, Dipl. Phys. ETH

Hess, Rolando, Dr.sc.nat. ETH

Lanker-Alimkoulova, Lisa, Dipl. Phys. Univ. Kasachstan

Lanker, Michael, Dipl. Phys. ETH

Le Pallec, Michel, Ph.D. Inst. Nat. Polytech. Grenoble

Leuthold, Jürg, Dipl. Phys. ETH
Occhi, Lorenzo, Dipl. El.-Ing. ETH
Schmid, André, Dipl. El.-Ing. ETH
Schneibel, Hanspeter, Dipl. El.-Ing. ETH
Solt, Katalin, Dr. sc.nat., ETH
Vélez, Christian, Dipl.Phys. ETH
Vogt, Werner, Dr. sc.nat. ETH
Wildermuth, Eberhard, Dipl. Phys. L.M. Univ. Munich
Zenklusen, Patrick, Dipl. El.-Ing. ETH

Technical Staff

Bolz, Edmund
Ebnöther, Martin
Graf, Christoph, Dipl. El.-Ing. HTL
Gu-Zhong, Ming, Dipl. El.-Ing. Chengdu Univ. P.R. China
Müller, Andreas

Administrative Staff

Bürgisser, Veronica
Dekker, Wendy

Microelectronics and Optoelectronics Laboratory

Prof. Dr. H. Melchior	Prof. Dr. G. Guekos
Tel. : +41 1 633 21 01	Tel. : +41 1 633 20 85
Fax : +41 1 633 11 09	Fax : +41 1 633 11 09
E-mail: h.melchior@iqe.phys.ethz.ch	E-mail: guekos@iqe.phys.ethz.ch

Institute of Quantum Electronics
Swiss Federal Institute of Technology
CH-8093 Zurich, Switzerland

<http://www.iqe.ethz.ch/me+oe/>

Thin Film Physics Group

Group Leader

Zogg, Hans, Dr. sc.nat. ETH, PD, Lecturer

Leader Photovoltaics

Tiwari, Ayodhya Nath, Dr. phil.sc. Indian Institute of Technology Delhi, India

Academic and Corporate Guests

Zimin, Dmitry Sergeevich, Yaroslavl, Russia, Exchange Student in Physics

Academic Staff

Alchalabi, Karim, Dipl.Phys. University of Freiburg, Germany

Bätzner, Derk Leander, Dipl.Phys. University of Cologne, Germany

Haug, Franz-Josef, Dipl.Phys. University of Ulm, Germany

Krejci, Martin, Dipl.Phys. ETH

Lai, Qun, Dr.sc.techn. ETH

Romeo, Alessandro, Dipl.Phys. University of Parma, Italy

Rudmann, Dominik, Dipl.Phys. University of Basel

Technical Staff

Leopold, Michael

Schreiber, Gerhard

Werner, Thomas

Administrative Staff

Pfammatter, Paulette

Thin Film Physics Group

Technopark ETH-Tract

Technoparkstrasse 1

CH-8005 Zürich, Switzerland

Tel. : +41 1 445 14 80

Fax : +41 1 445 14 99

E-mail: hans.zogg@iqe.phys.ethz.ch

RESEARCH SUMMARY

The research activities of the **Microelectronics and Optoelectronics Group** of Prof. Dr. Hans Melchior are oriented towards optoelectronics, device physics, and device technology. Component developments are mainly driven by applications in fiber optical communications and optical interconnects.

Studies in device physics include modeling of optical and optoelectronic properties of semiconductor optical amplifiers, investigations of optical switching phenomena in indium phosphide waveguides and basics for the design of optoelectronic components. For the realization of optical waveguide devices like Mach-Zehnder interferometers, laser diodes, semiconductor optical amplifiers, photodetectors and for high-speed electronics in indium phosphide, we rely on our own three-five compound semiconductor epitaxy and device processing technology. Our device technology capabilities include a metal-organic vapor phase epitaxy for indium phosphide and gallium arsenide compounds and a processing laboratory with contact photolithography, and facilities for wet and dry etching, evaporation and insulating materials deposition.

Our group is also involved in the design of optical fiber components in silica on silicon and in CMOS electronics for optical interconnects and in ultraviolet-photodiodes. These devices are customarily realized in commercial foundries.

Optical and electronic device design and characterization tools complement the physics, device, and technology activities.

Research highlights in 1999:

- Realization of optically controlled optical signal processing devices consisting of monolithic indium phosphide Mach-Zehnder waveguide interferometers with semiconductor optical amplifiers in their arms and demonstration of numerous applications.
- Demonstration of polarization independent 160 Gbit/s to 10 Gbit/s optical signal demultiplexing.
- Demonstration of simultaneous optical signal transmultiplexing from 40 Gbit/s to four separate 10 Gbit/s wavelength-channels.
- Demonstration of all-optical signal regeneration of 40 Gbit/s signals.
- Physical model established of the dynamics of Mach-Zehnder/semiconductor optical amplifiers and applied for accurate description of all-optical demultiplexing, wavelength conversion and signal regeneration in the 10 to over 100 Gbit/s domain.
- Arrayed waveguide filters in silica on silicon with flat-top passbands for polarization independent 16 channel wavelength division multiplexers.
- Exploitation of indium phosphide heterobipolar technology in high-speed optoelectronic circuits, including fully packaged high-performance 1,3 and 1,5 micrometer wavelength 10 and 40 Gbit/s receivers.
- Electronic driver- and receiver-arrays designed and realized in CMOS foundry demonstrating high-speed Gbit/s per link capabilities of CMOS-technology in optical interconnects.

Research highlights of the group of Prof. Dr. Georg Guekos:

- Application of four-wave mixing in semiconductor optical amplifiers for dispersion compensation, without the adverse effects of frequency shifting and phase mismatch at bit rates of 2.5 and 10 Gbit/s.
- Optical pulse generator using semiconductor optical amplifier in closed fiber loop, producing optical pulses of 5 picosecond duration with tunable repetition rates from 10 to 50 GHz and wavelengths tunable within 30 nm around 1550 nm.
- Dual-polarization, dual-mode external cavity diode laser set-up for penalty-free transmission of 200 Mb/s binary amplitude shift keying and 50 Mb/s binary phase shift keying signals over 25 km of optical fiber for fiber-optic antenna remote feeding.

The main activities of the **Thin Film Physics Group** under the leadership of PD Dr. H. Zogg and Dr. A.N. Tiwari are in the field of infrared sensors and thin film solar cells. Molecular beam epitaxy (MBE) grown heteroepitaxial PbTe and (Pb,Sn)Se layers on Si(111) are applied for thermal imaging arrays. For thin film solar cells, polycrystalline Cu(In,Ga)Se₂ (CIGS) and CdTe/CdS layers are grown by high vacuum evaporation on Si and GaAs substrates. Transparent conducting ZnO/ZnO:Al layers deposited by RF sputtering are employed for the thin film solar cells. In a project within the now terminated SSP “Optique II”, extremely wide bandwidth AlGaAs/CaF₂ quarter wavelength mirror stacks and saturable absorbers were developed for use in the generation of ultrashort laser pulses (see report of Prof. Dr. U. Keller).

Highlights of 1999:

Narrow bandgap materials for infrared sensors:

- One- and two-dimensional infrared sensor arrays for thermal imaging developed in PbTe on active Si-substrates which contain the read-out circuits.

Solar cell research:

- Development of flexible CIGS solar cells on lightweight polymer foils with a world record efficiency of 12.8%.
- CIGS “superstrate solar cells” with 8% efficiency developed, migration and accumulation of Ga on the ZnO interface detected.
- Recrystallization in CdTe and development of 12.5% efficiency solar cells by vacuum evaporation.

Educational Activities

The teaching activities of the Microelectronics and Optoelectronics and of the Thin Film Physics Group in 1999 included a two-semester course in Semiconductor Electronics and Integrated Circuits with device fabrication in the laboratory by H. Melchior, a course in Fiber Optical Communication and a course in Optoelectronics by G. Guekos and H. Melchior, a course in Semiconductor Lasers and Optoelectronics by H. Melchior, a course in Solar Cells by G. Guekos and R. Minder, a two-semester course in Electronics for physics students by G. Guekos and R. Zinniker and a two-semester course in Thin Film Physics and Technology by H. Zogg. The group is also actively involved in laboratory exercises of physics and electrical engineering students.

General Activities

During the year 1999 Prof. Dr. Hans Melchior had the honor of being President of the Laser and Electro-Optics Society (LEOS) of the Institute of Electrical and Electronics Engineers (IEEE). The Lasers and Electro-Optics Society, being very active worldwide in the promotion of scientific and application oriented publications and conferences, brought highly rewarding contacts with scientists and engineers throughout the world.

The Indium Phosphide and Related Materials (IPRM'99) Conference held from May 16th to 20th, 1999 in Davos was a major event for our group. We were conference organizers and also had several scientific presentations. This conference, it was its eleventh gathering, brings the major researchers in indium phosphide technology and indium phosphide electronic and optoelectronic devices together in a location that rotates between Europe, the Americas and Asia.

Besides numerous invited presentations at different conferences, Prof. Dr. Hans Melchior received the "Micro-Optics Award for Outstanding Technical Contributions to the Fundamentals and Applications of Micro-Optics" from the Micro-Optics Conference in Japan (MOC'99).

Prof. Dr. Georg Guekos from our group is active in presenting Switzerland in the management committee of the European Conference of Optical Communication (ECOC), the major European conference on fiber optical communication. He also represents Switzerland as Vice-Chairman in the Technical Committee of COST (European Cooperation for Scientific and Technical Research), an organization that promotes coordinated research in Europe. COST has 32 participating countries. The COST agreement was recently renewed by the Swiss Government.

Our three-five compound semiconductor technology and indium phosphide optoelectronic and electronic device development laboratory is intensively utilized by us and also by a number of other groups.

These users include the group of Prof. Dr. Eli Kapon of EPF-Lausanne, who regularly grows the epitaxial structures for his gallium arsenide quantum-well and quantum-wire lasers in our metalorganic chemical vapor deposition (MOCVD) facility.

Prof. Dr. Jerome Faist's group at the University of Neuchâtel utilizes our MOCVD for epitaxial regrowths in connection with his quantum cascade lasers.

Opto Speed S.A., a start-up company, that evolved from our group, relies extensively on our laboratory for the processing of their semiconductor optical amplifiers, photo-detectors, high-speed indium phosphide electronics and component packaging activities.

Prof. Dr. Heinz Jäckel of the Electrical Engineering Department of ETH is greatly increasing his use of the technology laboratory and also further developing our semiconductor optical amplifier and heterobipolar transistor technologies within his own research efforts.

Also, numerous research groups of the quantum electronics and solid state physics laboratories have found ways to use the technology laboratory to their advantage.

Low Pressure Metal Organic Vapor Phase Epitaxy for Three-Five Compound Semiconductors

E. Gini

Low pressure metal organic vapor phase epitaxy (LP-MOVPE) is used to grow III-V compound semiconductor materials with excellent control over their structural and electrical characteristics. The epitaxial growth of a III-V compound is achieved when column III metalorganic compounds react with hydrides of the column V elements at elevated temperatures over a single-crystal substrate. MOVPE permits a fine control of layer thickness, interface structure, material composition, and impurity concentration. Very thin structures can be grown for investigating quantum effects in dimensionally reduced systems.

At our Institute we have one MOVPE system installed with six hydride lines and eight metal-organic lines to satisfy the demands of the large variety of layer structures needed for the studied devices. The flexibility of our systems allows us to grow $\text{In}_{1-x}\text{Ga}_x\text{As}_y\text{P}_{1-y}/\text{InP}$ as well as $\text{Al}_x\text{Ga}_{1-x}\text{As}/\text{GaAs}$ structures in the same reactor. Layers with excellent purity (background doping around $10^{14}/\text{cm}^3$), layers for high performance active and passive optical devices, structures for high performance transistors, and AlGaAs quantum wires and dots are being grown.

For the characterization of the grown layers x-ray diffraction and room-temperature photoluminescence are routinely used. For the study of interface quality we have also access to secondary electron microscopy (SEM) and to transmission electron microscopy (TEM). Doping concentrations are determined either by Hall-measurements or by capacitance-voltage profiling.

In 1999 we made an upgrade of the gas detoxification system and improved the quality of the cleanroom atmosphere. The benefit from the reduction of particles was not only important for our purposes but also for the increasing number of external people which use layers grown with our MOVPE system. Thanks to our quality control we also grow layer structures for the spin-off company Opto Speed SA on a commercial base.



Photograph of our LP-MOVPE system with gas mixing cabinet, reactor and glovebox for loading (from left).

Plasma Etching

E. Gini

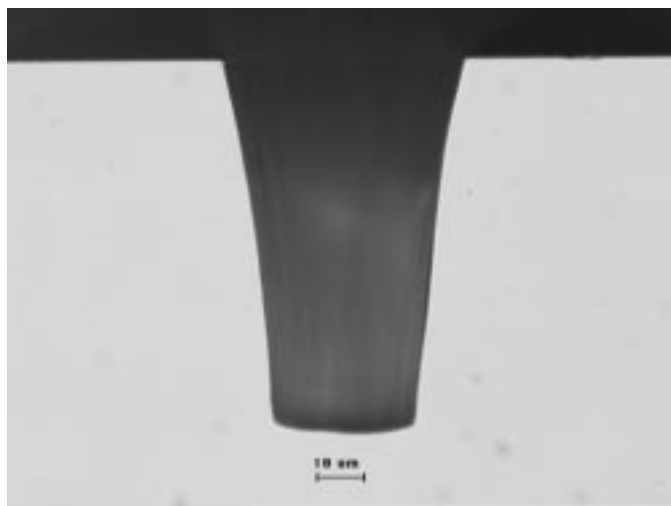
Plasma etching has become the dominating process for the patterning of III-V semiconductor based optoelectronic integrated circuits and is increasingly used also for microelectronic devices. At our Institute we use a variety of systems for dry etching. Commonly used are two conventional parallel plate reactors.

One system is exclusively used for the plasma etching of III-V compound semiconductors. The corresponding processes are based on mixtures of the gases H_2 , CH_4 and Ar. Process parameters as gas flows, chamber pressure, RF power density are optimized in order to achieve a high selectivity to the mask materials and a good homogeneity. We developed processes for the etching of InP, InGaAs, GaAlAs and InAlAs.

The same type of system is used for the dry etching of Ti and SiO_x layers using fluorine chemistry. These layers are used as mask material that are capable to withstand high temperatures. The etching of optical silica waveguides is done on the same system. We also etch $LiNbO_3$, polyimides, PMMA or ash organic residues with an oxygen plasma in this system. Both etching systems are computer controlled. A user-friendly menu allows people to run their dry-etching processes themselves without the need of profound technical knowledge.

In the case where high etching rates are needed (for example via holes) we use a magnetron enhanced reactive ion etching system (MIE). The magnetron allows a plasma at lower pressures than with conventional reactive ion etchers and gives raise to less damage of the samples due to ion bombardment. Thanks to a load-lock system that prevents the chamber from water vapor contamination, the system is also suited for chlorine based gas mixtures.

Etched structures are inspected by optical and electronic microscopy and the etch depth is determined by stylus force measurements (alphastep 200).

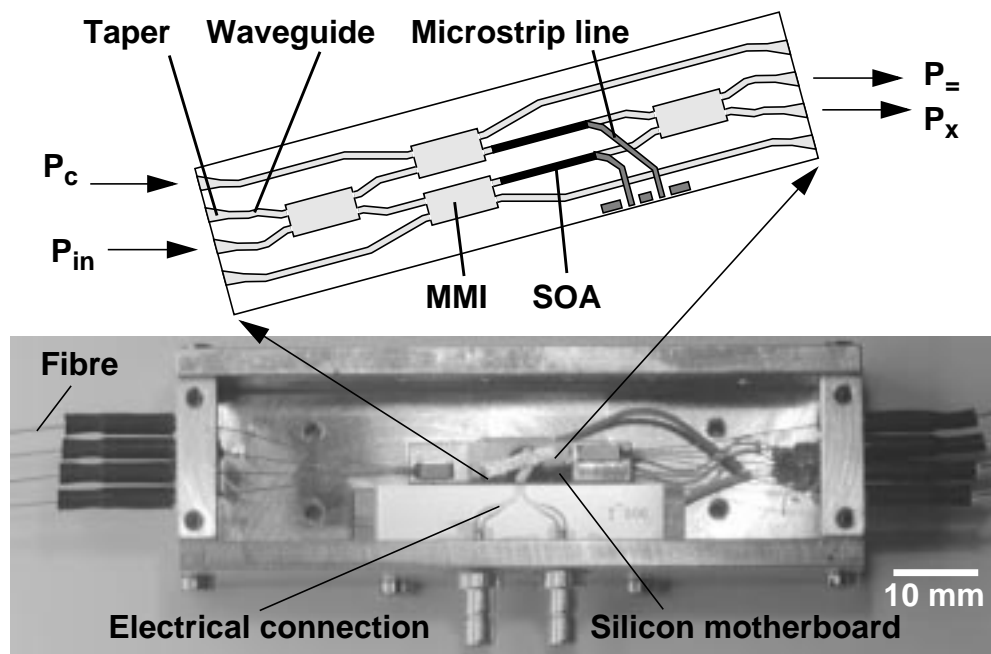


Cross-sectional view of a plasma etched via hole (80 μm depth) into an InP substrate.

All-Optical-Switches in Mach-Zehnder Configuration for Optical Communication Systems

W. Vogt, E. Gamper, M. Bitter, E. Gini, W. Hunziker, H. Melchior

High-speed all-optical-switches using group III-V semiconductors will play an important role in future optical communication systems. Our all-optical-switches operate in the 1.55 micrometer wavelength range. They consist of monolithically integrated InGaAsP/InP semiconductor optical amplifiers (SOA's), optical waveguides and multimode interference couplers (MMI) in a Mach-Zehnder interferometer (MZI) configuration. Introducing a short optical control pulse P_c into one arm of the MZI results in a dynamic change in the carrier population of the SOA that changes the refractive index of the MZI. Due to the resulting phase difference in the two MZI arms, the optical signal P_{in} is switched from output P_- to output P_x . Inside the device, the optical signals are guided from and to the different elements by straight and curved waveguides. Integrated mode shape adapters provide efficient coupling of the optical signals to optical fibres. The waveguides at the facets are tilted and antireflection coated to reduce back reflections. A flip-chip packaging technique that combines electrical interconnections and self-aligned optical coupling between waveguides and arrays of single-mode fibres has been developed. The device is soldered upside down (flip-chip) onto a Silicon motherboard. The motherboard also serves as mounting platform for the arrays of single-mode fibres. This mounting technique guarantees a stable optical interface between all-optical-switch and fibres.



All-optical switch consisting of semiconductor optical amplifiers (SOA), 3 dB splitters / combiners (MMI), waveguides and modeshape adapters (Taper).

(Top: schematic view of an all-optical switch, bottom: fabricated module)

All-Optical Switches with Monolithically Integrated Phase Shifters

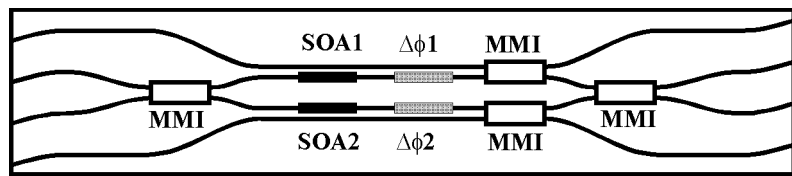
E. Gamper, W. Vogt, M. Bitter, E. Gini

Optical signal processing is an approach that holds the promise to overcome the speed limits of electrical signal switching in high speed optical communications. We realized multi-purpose all-optical switches with monolithically integrated phase shifters, based on Mach-Zehnder interferometer/semiconductor optical amplifier structures.

These switches are capable to perform demultiplexing of optical data streams from high to low data rates. Furthermore, they can be used as wavelength conversion devices to shift optical signals from one wavelength to another. Another application of the devices is in signal conditioning to re-shape and re-time optical data.

For all these applications, indium phosphide Mach-Zehnder interferometer/semiconductor optical amplifier devices are advantageous, especially if they contain monolithically integrated phase shifters. These phase shifters are useful for electronic channel switching and for the selection of channels after all-optical switching.

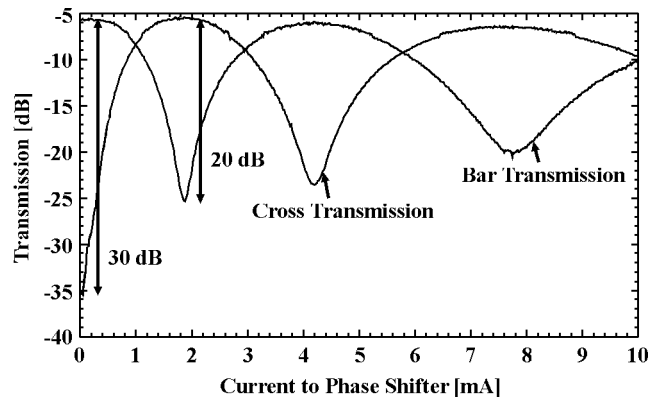
The monolithically integrated devices are based on Indium Gallium Arsenide Phosphide (InGaAsP) on InP. They feature waveguides that interconnect the light between the splitters and combiners and the nonlinear optical elements in the Mach-Zehnder interferometer arms, namely the semiconductor optical amplifiers (SOA's) and phase shifters ($\Delta\phi$).



(100) InP

Mach-Zehnder interferometer switch combining semiconductor optical amplifiers (SOA's), phase shifters ($\Delta\phi_1$, $\Delta\phi_2$) and multi-mode interference (MMI) couplers.

The phase shifters allow high static extinction ratios at gating occurs of only 2 mA.



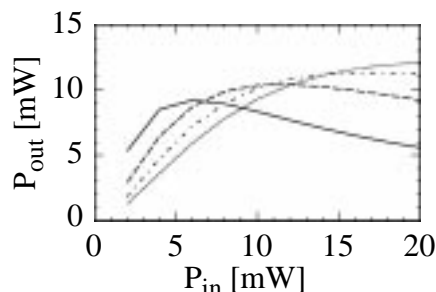
Electrical switching characteristics Mach-Zehnder interferometer/semiconductor optical amplifier switch with monolithically integrated phase shifters.

All-Optical Mach-Zehnder Interferometer Modeling

M. Caraccia-Gross and H. Melchior

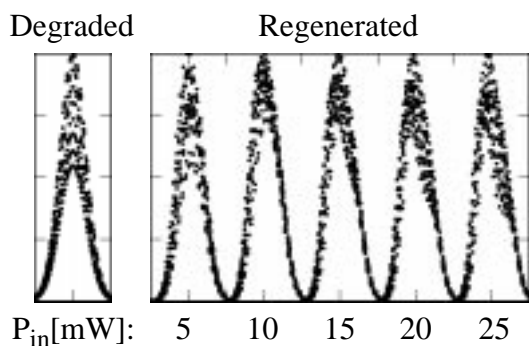
A model has been developed to describe all-optical operations - such as e.g. wavelength conversion and optical time demultiplexing - of monolithically integrated Mach-Zehnder interferometers (MZI) with semiconductor optical amplifiers (SOA's) in their arms. The model includes gain compression, as well as wavelength dependence of the gain and of the amplified spontaneous emission in the SOA's. The optical properties of the multimode interference couplers are included to describe the signals propagation through the entire MZI-SOA.

We show here simulation of 3R (re-shaping, re-amplification and re-timing) regenerative 10 GHz wavelength conversion, demonstrating the advantage of using MZI-SOA's to complete wavelength conversion simultaneously with 3R regeneration. In all the results presented here the pump and the probe are 10 GHz signals with pulses of 20 ps duration. We first show the simulated wavelength conversion transfer function.

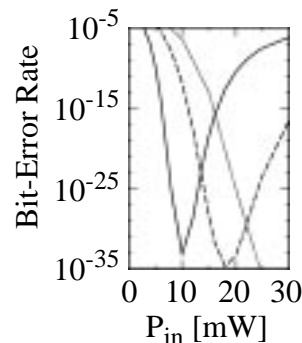


It allows to estimate the best pump power to choose to get minimal output amplitude fluctuation in case of input amplitude fluctuation. Next we show the same operation, but with a pump signal whose amplitude fluctuation obeys a distribution $N(\bar{P}, \sigma)$ corresponding to a quality factor $Q = \bar{P}/\sigma$ of 3.9, leading to a bit-error rate $BER \approx \exp(-Q^2/2)/Q\sqrt{2\pi}$ of $5E-5$. The normalized eye diagrams of the input degraded and of the output regenerated signals are shown below for different pump powers and for a 10 mW probe power. We observe that the pump signal is best reshaped for a 10 mW pump power. The BER are calculated from these eye-diagrams and traced as function of the pump power. We observe that the lowest BER, i.e. the best BER, is at lower input pump power for lower probe power, but that one gets better BER's with higher probe powers

Wavelength conversion transfer function. Probe power is 10 (plain), 20 (dash), 30 (dash dot) and 40 (dot) mW.



Eye diagrams of the degraded and regenerated signals. The input pump powers are 5 to 25 mW. The 10 GHz probe's power is 10mW.



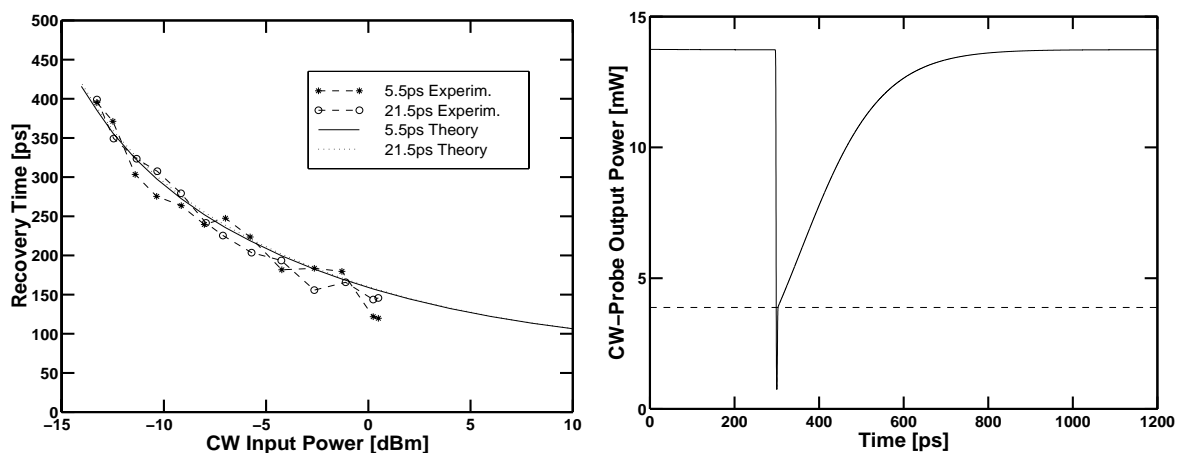
Bit-error rate vs pump power. 10GHz probe is 10 (plain), 20 (dash) and 30 (dot) mW.

Nonlinear Dynamics Simulations and Measurements in Semiconductor Optical Amplifiers.

R. Gutiérrez-Castrejón, L. Schares, G. Guekos

An adequate theoretical model to simulate the dynamical behaviour of a photonic device is useful for project planning, testing, and interpretation and extrapolation of experimental results. With this motivation in mind we have developed a set of algorithms that simulate the gain and refractive index evolution of a semiconductor optical amplifier when one or several co-propagating electromagnetic pulses interact with the active medium. Our simulation tools follow a frequency domain approach. This guarantees accuracy, efficiency (in computer time and memory) and flexibility to study different nonlinear dynamical processes, namely, non-degenerate four-wave mixing, cross-gain modulation, cross-phase modulation, and others. Semiconductor optical amplifiers using these light-matter interactions find applications in the telecommunications domain, for instance, as the key elements for switching and wavelength conversion.

Although our algorithms are limited to the interaction of copropagating beams, they take into account the effect of gain dispersion, energy inter- and intra-band processes, and we are on the way to incorporate the effect of amplified spontaneous emission. They have been able to successfully reproduce measurements of gain recovery time in a 0.5 mm long bulk semiconductor optical amplifier. We expect to promptly extend the simulation capabilities to study a 1.0 mm long device. Curves of gain recovery time and modulation depth against saturation level have also been calculated considering the cases whether the gain compression produced by ultra-fast effects (carrier heating (CH), spectral hole-burning (SHB)) can or cannot be detected by the experimental set-up.



Measured and calculated gain recovery time v.s. saturation level for two pump pulse-widths FWHM: 5ps (solid line) 21.5ps (dotted line).

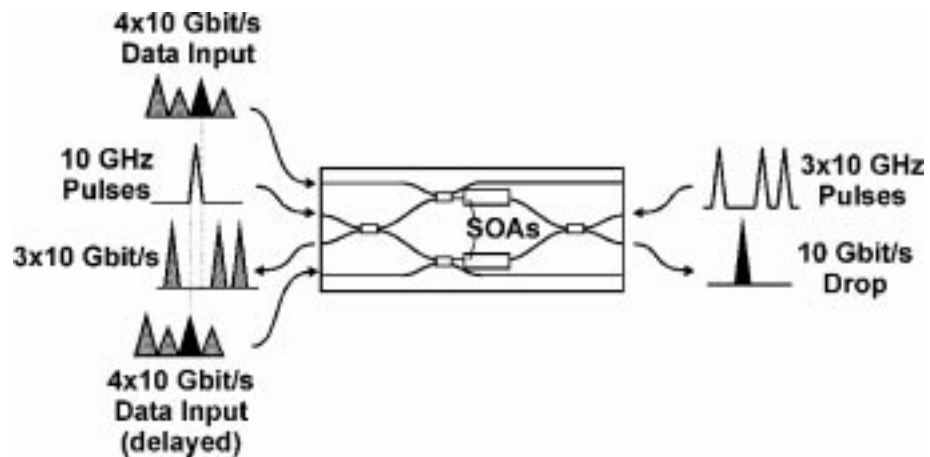
Typical evolution of a transmitted probe beam power when a 2 ps pulse is injected. Below the dashed line the gain compression is mainly due to SHB and CH.

Novel Concept for All-Optical Add/Drop Multiplexing with Regenerative Capability

St. Fischer, M. Dülk, E. Gamper, W. Vogt, W. Hunziker, E. Gini, H. Melchior

Demultiplexing and add/drop multiplexing are amongst the key functions required within a optical time division multiplexed (OTDM, means different channels temporally interleaved) network nodes. In the add/drop multiplexer one channel has to be completely extracted out of the incoming data stream while leaving the remaining channels undisturbed. A new channel can be added into this cleared time slot by a passive coupler and the appropriate time delay. Simultaneous good dropping and complete clearing are indispensable to guarantee further error-free data processing because insufficiently suppressed pulses can cause interference noise while adding a new channel into this vacant time slot.

A novel concept for perfect clearing and dropping including data regeneration capability at 40 Gbit/s has been demonstrated in collaboration with the Technical University of Denmark



using a monolithic Mach-Zehnder interferometer (MZI) with integrated semiconductor optical amplifiers (SOA). The basic idea is founded on two counter-propagating probe pulse streams which are all-optically modulated by the MZI-SOA. One stream consists of high-quality 10 GHz pulses forming the base for drop channel (black). The other stream consisting of 3x10 GHz pulses forming a 40 GHz stream with an empty time slot. On this stream the data of the three remaining channels are imposed (gray). Due to the empty time slot in the 3x10 GHz probe stream the drop channel is automatically ignored and is therefore perfectly removed out of the remaining channels. The same applies for the drop channel which is furthermore simplistically extracted due to its different propagation direction.

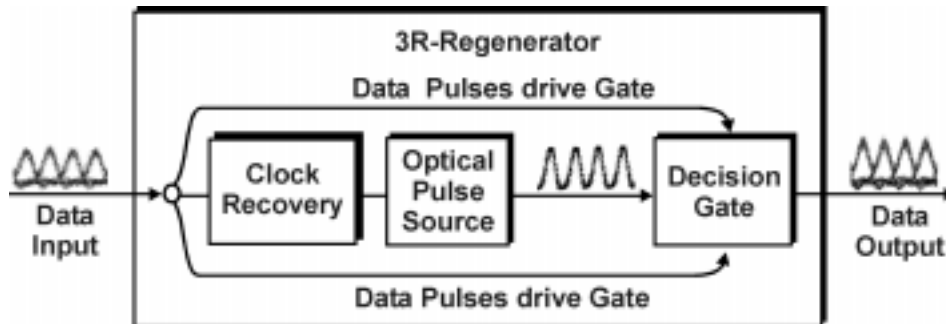
Bit error rate measurements have been performed showing a low penalty of only 2 dB for the dropped 10 Gbit/s channel as well as for the remaining 3x10 Gbit/s channels. Adding a 10 Gbit/s channel into the emptied time slot showed no extra penalty which demonstrates the perfect clearing functionality.

References: St. Fischer, M. Dülk, et al., accepted for publication in *IEEE Photon. Techn. Lett.*

Optical Data Regeneration at 40 Gbit/s

St. Fischer, M. Dülk, E. Gamper, W. Vogt, W. Hunziker, E. Gini, H. Melchior

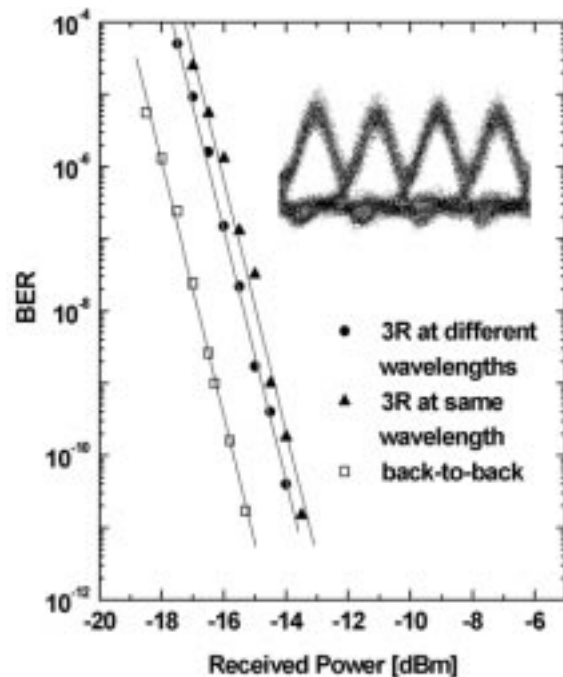
In optical high-capacity networks, accumulation of impairments of optical signals due to long-haul transmission or signal processing at network nodes require periodical restoration of the data. Optical 3R regeneration (*Reamplification, Reshaping and Retiming*) is an interesting alternative to electronic regeneration, allowing significant reductions of timing jitter and amplitude noise after long transmission spans. It thereby allows optical signals to be maintained in the optical domain over long transmission distances and through network nodes.



Schematic view of a 3R regenerator with its basic three units.

Optical 3R regenerators consist of a clock recovery unit, an optical pulse source and an all-optical decision gate. The clock recovery unit extracts the repetition rate of the deteriorated data and drives the optical pulse source which produces high-quality optical clock pulses at exactly this rate. This pulse stream is then on-off modulated by the data signal in the decision gate.

A 3R-regeneration at 40 Gbit/s has been performed in a collaborative experiment with British Telecom using an integrated Mach-Zehnder interferometer in connection with an electronic clock recovery and a compact pulse source. The results are summarized in the bit error rate (BER) graph on the right side demonstrating a low penalty of less than 2 dB for the regenerated data in respect to the back-to-back measurement (transmitter and receiver alone). The insert shows the regenerated 40 Gbit/s output eye diagram indicating the good separation of the 1s and the 0s.

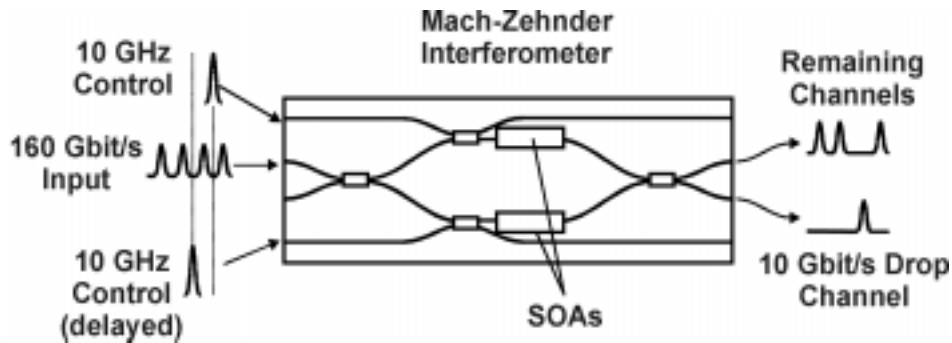


Reference: St. Fischer, M. Dülk, et al., *Electron. Lett.*, **35**, (23), 2047, (1999)

Ultra-fast All-Optical Demultiplexer for 160 Gbit/s Networks

St. Fischer, M. Dülk, E. Gamper, W. Vogt, H. Hunziker, H. Melchior

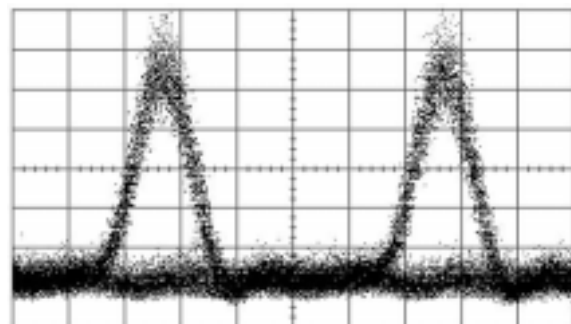
Future ultra-high speed optical networks will exploit optical time division multiplexing (OTDM, means different channels temporally interleaved) with data rates of up to 160 Gbit/s per wavelength. Consequently, optical devices in network nodes like add/drop multiplexers or demultiplexers are requested to process these data rates. The task of demultiplexers is to drop one channel out of the high-speed OTDM data stream for further data processing or routing at lower speed.



Principle of 160 to 10 Gbit/s demultiplexing using a Mach-Zehnder interferometer module

A 160 to 10 Gbit/s all-optical demultiplexing experiment has been performed in collaboration with the Technical University of Denmark using a monolithic Mach-Zehnder interferometer with integrated semiconductor optical amplifiers (MZI-SOA). Therefore, the 160 Gbit/s data stream is launched into the input port of the MZI-SOA. Two 10 GHz control pulse sequences with the proper delay in respect to each other switch the 160 Gbit/s data stream from one output to the other and back again. This periodic switching results in the dropping of one 10 Gbit/s channel out of the 160 Gbit/s stream. The clear and open eye diagram of the 10 Gbit/s drop channel is shown in the figure below. It demonstrates good separation of the 1s and the 0s and proves the modules fast switching capability for high-speed networks.

Eye diagram of the 10 Gbit/s drop channel, extracted from the 160 Gbit/s OTDM stream

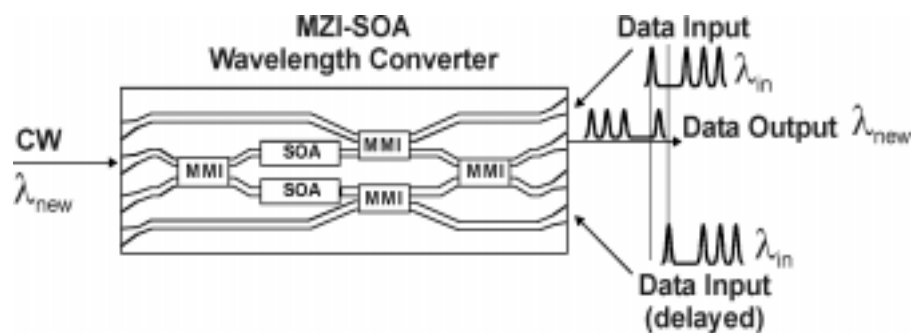


References: St. Fischer, M. Dülk, et al., *submitted to Electron. Lett.*

All-optical wavelength conversion at 10 Gbit/s over extended 80 nm wavelength range

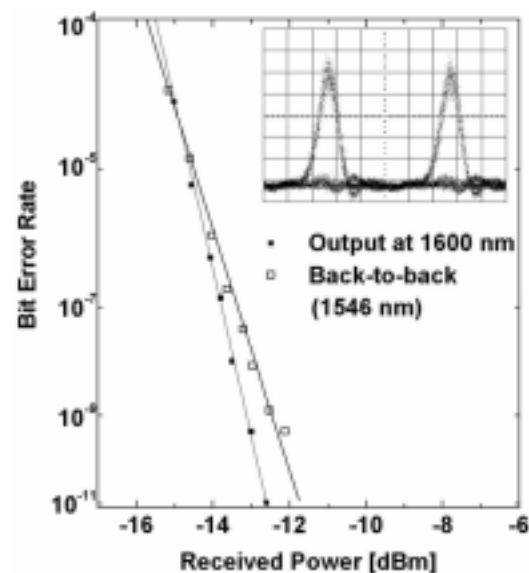
M. Dülk, St. Fischer, E. Gamper, W. Vogt, W. Hunziker, E. Gini, H. Melchior

To satisfy the increasing demand for bandwidth in optical networks, wavelength-division multiplexed (WDM) systems will not only use the standard 1530 to 1565 nm (C-band) wavelength range of standard Erbium doped optical fiber amplifiers but also the 1565 to 1610 nm wavelength range (L-band) of new optical amplifiers. Therefore, to route traffic through optical network nodes, optical wavelength converters are thus needed to cover this full 80 nm span. Since the data passes numerous network nodes before reaching the user, regenerative capabilities are an important feature of such wavelength converters.



Operation principle of MZI-SOA wavelength converter

Our wavelength converters, that use a cross-phase modulated Mach-Zehnder interferometer (MZI) with integrated semiconductor optical amplifiers (SOA's), have been modified to cover this extended wavelength span. In the experiment, a 10 Gbit/s signal at 1546 nm has been wavelength up- and down-converted within the entire C- and L-band span. The wavelength converted output signals exhibit very low noise and chirp that has been demonstrated by an 80 km transmission experiment in the L-band at 1600 nm. The low noise characteristics, as well as the regenerative capabilities, originate from the interferometric structure of this wavelength converter and is accompanied by a negative penalty and steep bit error rate curves. The inset shows the eye diagram of the 10 Gbit/s converted output signal.



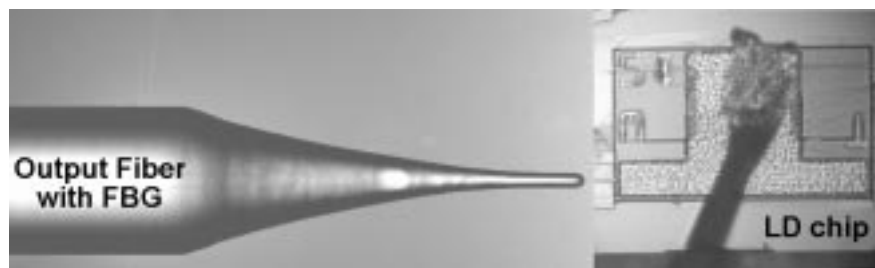
References: M. Dülk, St. Fischer, et al., accepted for publication in *Electron. Lett.*

Mode-locked laser diodes with external fiber Bragg grating cavity

M. Dülk, H. Melchior

Optical pulse sources are key components for high-speed optical networks. Qualities needed are short optical pulses, high repetition rate, precisely chosen wavelength, low timing jitter and synchronization capabilities to the external clock of the electrical network components. Actively mode-locked lasers are promising candidates featuring these requests.

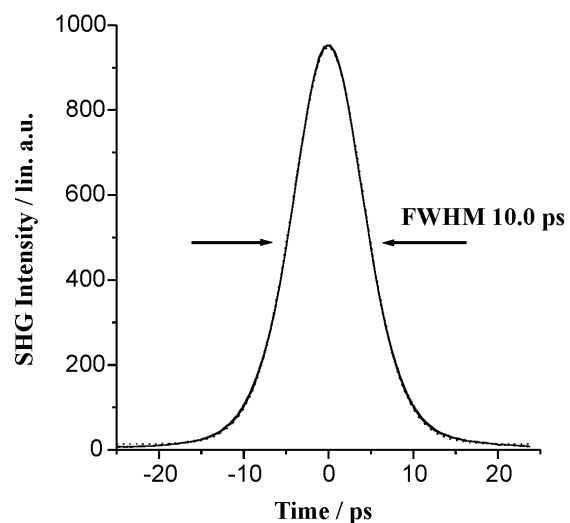
We have realized a hybrid external cavity laser with a round-trip frequency of 9.95328 GHz, corresponding to the communication network standard STM64. As laser we use an InGaAsP/InP ridge waveguide laser diode (LD) of a length of 250 μm with anti- and high-reflection coatings at the facets. The diode has been additionally provided with a saturable absorber fabricated by heavy ion implantation. The light output of the laser diode is partially reflected back by a broadband non-apodized fiber Bragg grating (FBG) for optical feedback and wavelength selection. The center wavelength is 1552.4 nm, the 3dB optical bandwidth of the Bragg grating is 2.4 nm which is sufficiently broad for pulses with duration of about 2 ps. The position of the FBG inside the fiber defines the longitudinal mode spacing of the laser cavity which has to match the desired modulation frequency of STM64.



Laser diode (LD) with external fiber Bragg grating (FBG)

With this external cavity set-up, transform-limited short optical pulses with a duration of 6.5 ps FWHM, sech^2 shape and an extinction better than 25 dB have been generated at a repetition rate of 10 GHz. Center wavelength is 1552 nm.

Measured auto-correlation trace of 10 GHz mode-locked optical pulses with 10.0 ps FWHM. The Levenberg-Marquardt fit (dotted line) demonstrates perfect sech^2 pulses with 6.5 ps duration



Saturable absorbers realized by heavy ion implantation for mode-locked semiconductor laser diodes

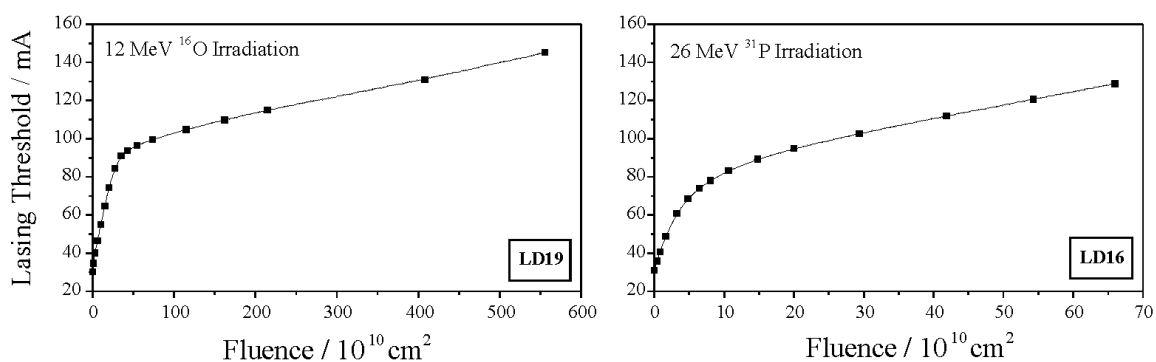
M. Dülk, H. Melchior

Semiconductor lasers are key components in optical fibre communication systems. Due to their small size the modulation bandwidth usually exceeds 10 GHz, which makes them attractive as optical pulse or clock sources. Mode-locked semiconductor lasers with saturable absorbers exhibit superior optical pulse quality like chirp-free narrow pulses with very good extinction ratio. The aim of this investigation was to create saturable absorbers in bulk semiconductor laser diodes by MeV ion bombardment.

The semiconductor laser diodes were ridge waveguide lasers with an overall length of 250 μm and with an InGaAsP bulk active layer of 110 nm thickness. Initial lasing threshold was 29 mA, the gain peaked at a wavelength of 1550 nm. Ion implantation allows to fabricate an absorbing section inside the active layer with a width of some tens of microns. The targeted ion range is five to ten microns from the laser facet whereas the damage to the facet should be kept as low as possible.

Oxygen with an energy of 12 MeV and phosphorus ions with an energy of 26 MeV were chosen as good candidates for producing optically absorbing layers with the appropriate width and depth. Several laser diodes with equal initial output characteristics have been bombarded by successive doses of P or O ions, respectively. Immediately after each irradiation, the laser diodes were characterized.

The dependence of various laser parameters, like lasing threshold, internal quantum efficiency, wavelength shift and others, on the ion fluence has been investigated. For both ion species, the lasing threshold increases with a functional dependence of the form $1 - \exp(-F/F_0)$ as a function of the fluence F up to a certain dose F_0 . For higher fluences a linear increase is observed. As expected from the simulated number of displaced atoms per implanted ion, the saturation takes place faster for the phosphorus bombardment.

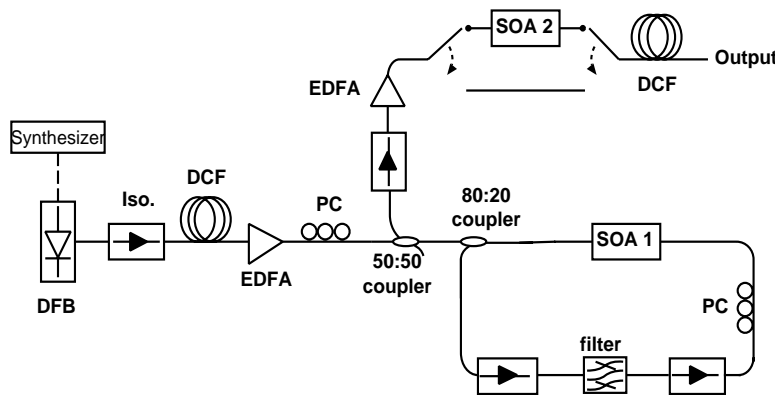


Dependence of lasing threshold on the fluence for phosphorus and oxygen ion implantation

Wavelength-Tunable Pulse Source at 5-40 GHz by Optical Modulation of a Semiconductor Optical Amplifier in a Fibre Ring Laser

L. Schares, R. Gutiérrez-Castrejón and G. Guekos

Short optical pulse sources operating at high repetition rates are key components in high-speed optical communications networks and all-optical logic circuits. Its broad wavelength tunability is a highly desirable feature in WDM applications. A convenient method for generating short pulses is based on active mode-locking in fibre ring lasers (FRL). The use of a semiconductor optical amplifier as active medium in the ring is attractive, since it can provide both gain over a broad wavelength range and modulation due to its fast gain (and phase) dynamics.

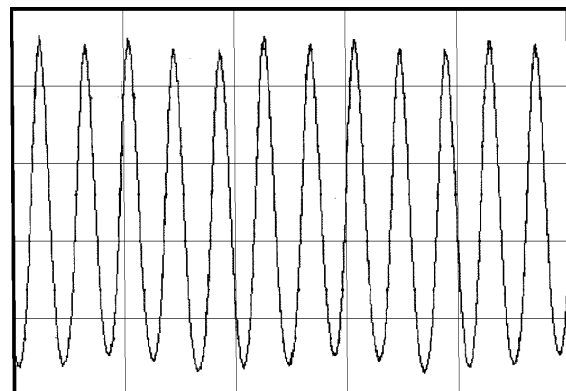


Experimental Setup of the Fibre Ring Laser. SOA 1 is optically modulated by the seeding pulses. SOA 2 may be used to reduce a 5 GHz amplitude modulation of the output pulse train.

We have set up a harmonically mode-locked FRL, based on optical modulation of a SOA by 5 GHz seeding pulses, delivered by a gain switched DFB laser. Fast gain saturation together with relatively slow recovery form a short temporal window within which the mode-locked pulses may form.

When the frequency, f_{ext} , of the seeding pulses is adjusted to the N_{th} harmonic of the ring oscillator f_{ring} , a mode-locked pulse train at about 5 GHz is generated. A larger repetition rate of $n f_{ext}$ can also be obtained by setting $f_{ext} = (N+1/n) f_{ring}$ (with $n > 1$). In particular we have achieved up to 8 times frequency multiplication, from 5 to 40 GHz. In this case an almost constant pulsewidth of 3.8-4.3 ps after dispersion compression was observed over more than 30 nm wavelength tuning range.

25 GHz pulse train (100 ps/div.)



Chirp Dynamics in Wavelength Conversion using Semiconductor Optical Amplifiers

L. Occhi, L. Schares, R. Gutiérrez-Castrejón and G. Guekos

All-optical wavelength converters can become key elements in future optical networks employing wavelength division multiplexing (WDM). They have the potential to resolve wavelength congestion at the network nodes.

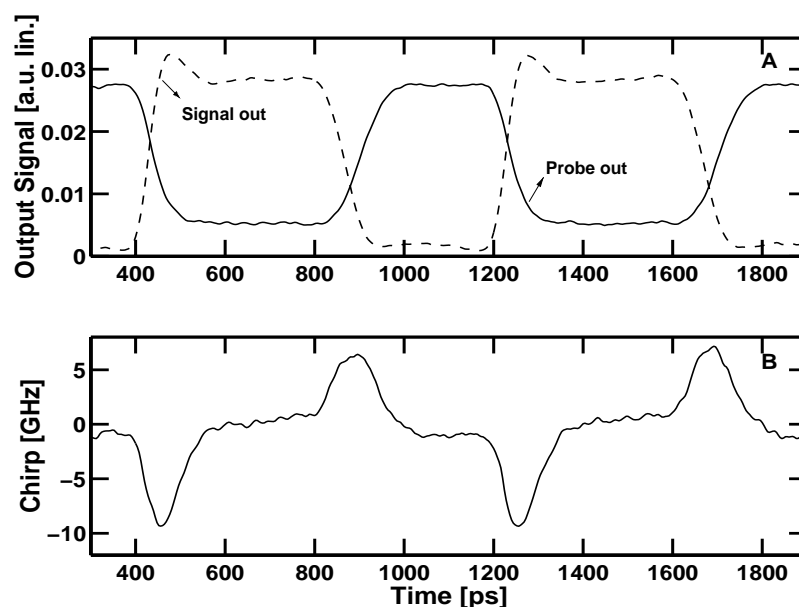
Wavelength conversion can be achieved using nonlinear effects in Semiconductor Optical Amplifiers (SOA's) in three different ways: cross-gain modulation (XGM), cross-phase modulation (XPM) and four-wave mixing (FWM).

One important parameter to judge the quality of the converted signal is its chirp, i.e. the instantaneous deviation of the optical signal frequency.

We are investigating the dynamics of the chirp induced by SOA's used as wavelength converters. Typical waveforms at the SOA output in the case of XGM are illustrated below. Two beams are injected in the SOA: the signal that modulates the gain of the SOA, and the probe that is a cw beam at a wavelength to which the signal will be converted. The SOA-gain is modulated by the signal and consequently the probe at the output becomes an inverted replica of the signal (Fig. A). The gain modulation is accompanied also by a phase modulation, which chirps the probe. Fig. B shows the chirp of the probe as a function of time. Typical in XGM is the positive chirp of the probe, i.e. a blue shift during the rising edge and a red shift during the falling edge of the probe.

The investigations show that wavelength conversion based on XGM is always accompanied by signal chirp. The chirp deteriorates the signal quality and can be minimized by increasing the optical power of the probe.

Wavelength Conversion by XGM. (A) signal and probe power as a function of time. (B) Chirp of the probe as a function of time. $\lambda_{\text{probe}} = 1549.9 \text{ nm}$, $\lambda_{\text{signal}} = 1554.9 \text{ nm}$.



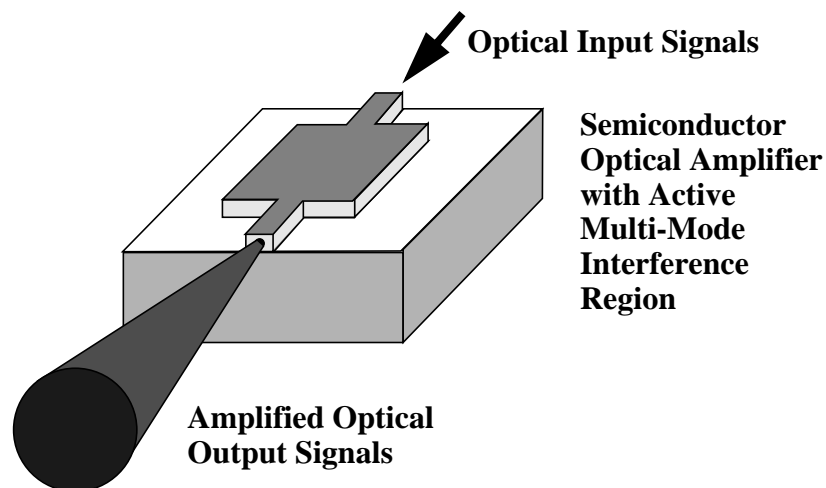
Active Multi-Mode-Interferometer Semiconductor Optical Amplifier

K. Hamamoto, E. Gini, C. Holtmann, and H. Melchior

Enormous demands for capacity growth of telecommunications is continuing to increase world-wide. Optical telecommunication systems are spreading into local-areas presently, and semiconductor optical amplifiers (SOA's) are one of the key-devices for such purposes.

We have already demonstrated, that laser diodes which exploit the concept of multi-mode interference type active structures are capable of increased kink-free saturated output powers.

Here we also explore the concept of multi-mode interference in the active sections of semiconductor optical amplifiers. Active multi-mode interference regions allow optical input signals that are amplified in large active areas to be refocussed and superimposed into a coherent output beam. We expect this active multi-mode interference amplifier concept to be a key-technology for semiconductor amplifiers.



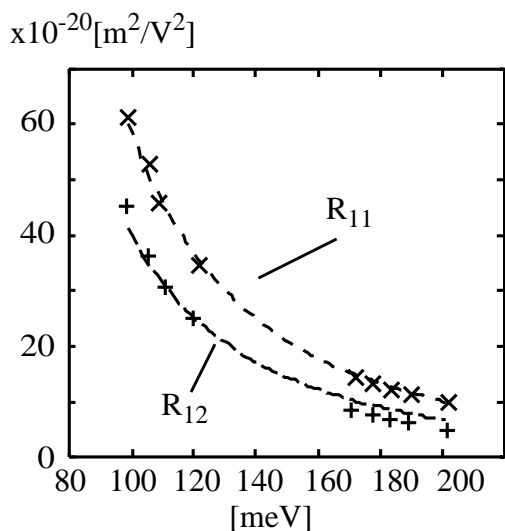
Schematic view of Semiconductor Optical Amplifier in active multi-mode-interferometer configuration.

Analysis of Electro-Optic Effects in InP / InGaAsP Based Waveguide Structures

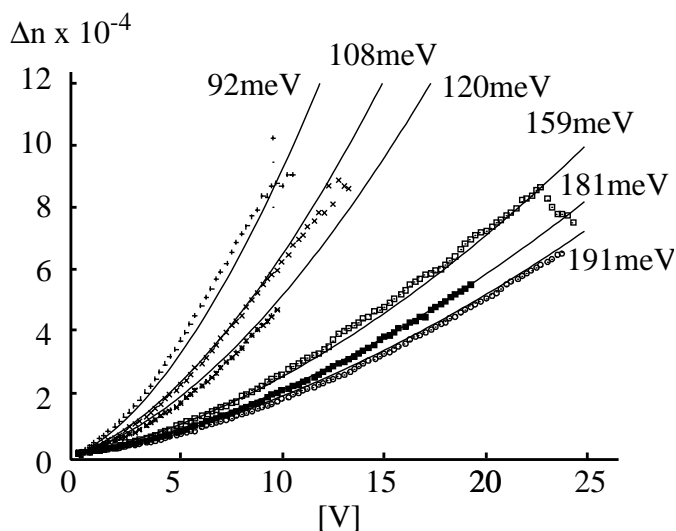
G. Hagn

The most important electro-optic nonlinear effects in a reverse biased pin-diode are the Franz-Keldysh effect, the Pockels effect and the carrier depletion effect. Electro-optic effects in InP/InGaAsP were examined by analysing the switching behaviour of Mach-Zehnder interferometers. The phase shifting arms of the interferometer are implemented as pin-diodes oriented under various angles with respect to the $[0\bar{1}1]$ crystal axis. The electric fields necessary to change the refractive index are generated by reverse biasing the pin-diodes. The Pockels effect can be separated from the other effects by using its $\cos(2\phi)$ angular ϕ dependency with respect to the $[0\bar{1}1]$ crystal axis. The coefficients of the electro-optical effects were obtained by comparison of the measured refractive index change with the average of the electric field averaged with the optical mode.

Detailed knowledge of the electro-optic coefficients is essential for the design of optimized electro-optic space switches. It allows to maximise the efficiency of the effects, and thereby switching voltages low, while maintaining polarisation insensitivity and keeping the optical losses within acceptable limits. Low switching voltages are required for high speed switching. This is important as electrically controlled optical space switches are key components for use in practical optical communication networks, where they can perform fast switching, rerouting and channel add-drop functions. The InP/InGaAsP material system is of special interest because it allows monolithic integration of space switches, lasers, amplifiers and photodetectors.



Measured coefficients and theoretical curve of the Franz-Keldysh electro-optic effect



Refractive index changes versus applied voltage measured and calculated for various photon energies with respect to the bandgap energy in InGaAsP in meV

High Output Powers from Semiconductor Laser Diode Arrays Coherently Coupled in Mach-Zehnder Configuration

Ch. Vélez and H. Melchior

High single-mode optical powers coupled into single-mode fibers are a key for many applications in optical communications, meteorology, medical surgery and laser machining.

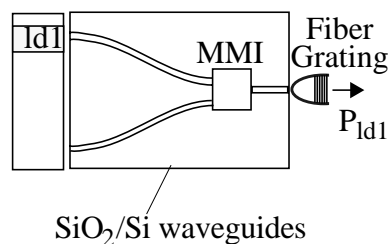
Towards this end, we are exploring the coherent coupling of semiconductor laser diode arrays in Mach-Zehnder Interferometers (MZI) consisting of SiO₂/Si waveguides and Multi-Mode Interference Coupler (MMI), and an external fiber grating.

In the case where two laser diodes are coupled coherently the total output power P_{tot} adds up to:

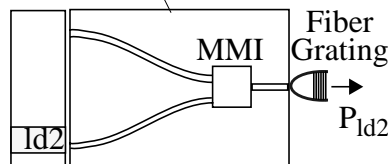
$$P_{tot} = \frac{1}{2} \cdot (P_{ld1} + P_{ld2} + 2 \cdot \sqrt{P_{ld1} \cdot P_{ld2}} \cdot \cos(\phi_1 - \phi_2)).$$

If only one laser diode is operative the output power is just $P_{ld1} = \frac{1}{4} \cdot P_{tot}$. As shown in the adjoined figures, we were able to show that such a hybrid laser-array operating at a wavelength of 980 nm is able to coherently couple light into a single mode-fiber, thereby achieving high single-longitudinal mode output powers.

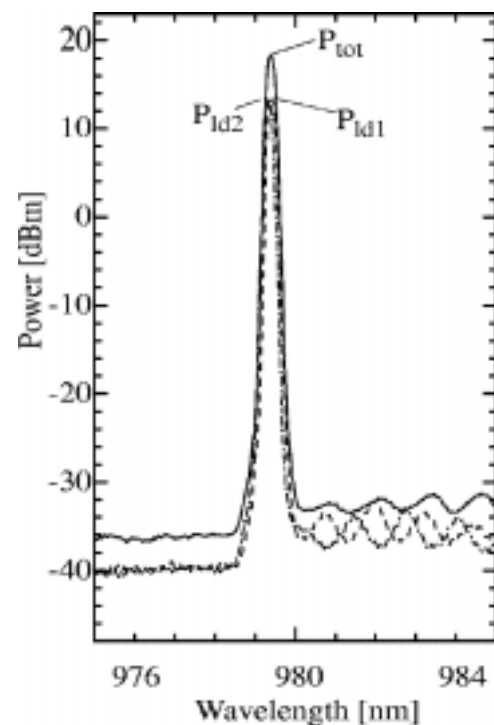
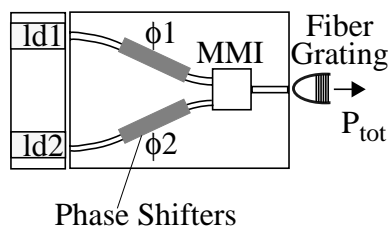
Laser diode (ld1) coupled to MMI and fiber grating: Output spectrum shows single-longitudinal mode (spectral resolution of spectrometer is 0.2nm).



Laser diode (ld2) coupled to MMI and fiber grating: Output spectrum shows single-longitudinal mode.



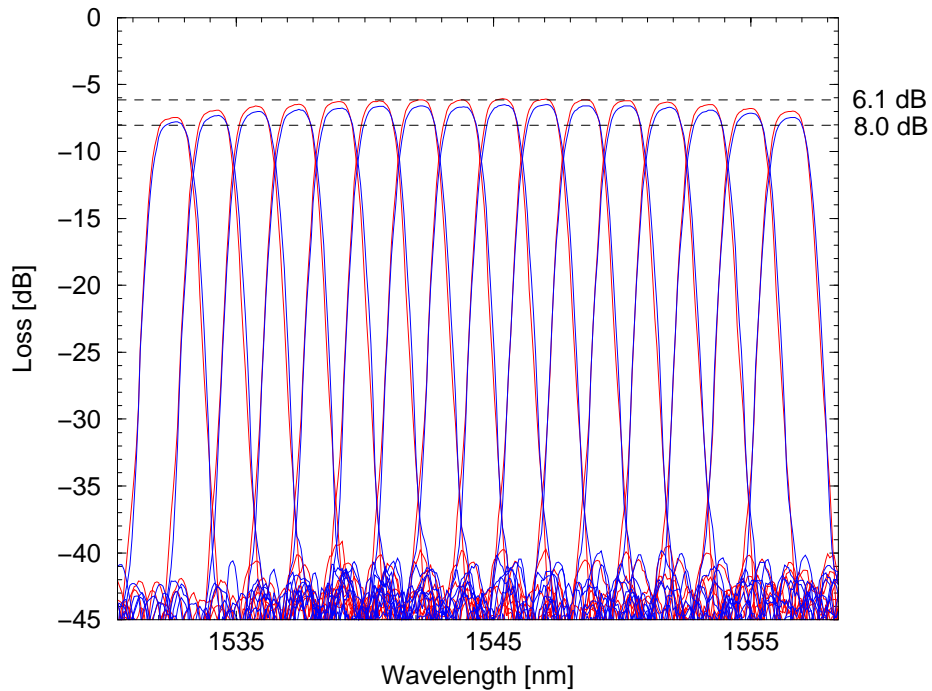
Two laser diodes coupled to MMI and fiber grating: Provided phase adjustment ϕ_1 and ϕ_2 is optimized, outputs add to single-longitudinal mode of high power.



Silica-on-Silicon Multi-Channel Phased Array Wavelength Filters

E. Wildermuth, M. Lanker, and H. Melchior

High-capacity multi-wavelength fiber-optical communication systems need special wavelength multiplexer and demultiplexer filters that are polarization insensitive, have low losses and low crosstalk as well as passbands that are tolerant to deviations of the channel wavelengths. Filters of our design that were realized in a foundry for silica-on-silicon optical waveguide components meet the stringent requirements, including standardized frequency allocations.



Parameter	SiO ₂ /Si Wavelength Division Multiplexer	Unit
Number of Channels	16	
Channel Spacing	200	GHz
Wavelength Region	1530-1560	nm
Loss (Fiber-to-Fiber)	6.1 (minimal), 7.9 (typical)	dB
Optical Crosstalk	< -34.9	dB
Uniformity	0.5 (minimal), 0.9 (typical)	dB
1 dB Bandwidth	1.00 (63% of channel spacing)	nm
3 dB Bandwidth	1.38 (86% of channel spacing)	nm
Polarization Shift	0 (minimal), 0.04 (typical)	nm
Polarization Dependent Loss	0.2 (minimal), 0.5 (typical)	dB
Temperature Dependence	0.01	nm/°C

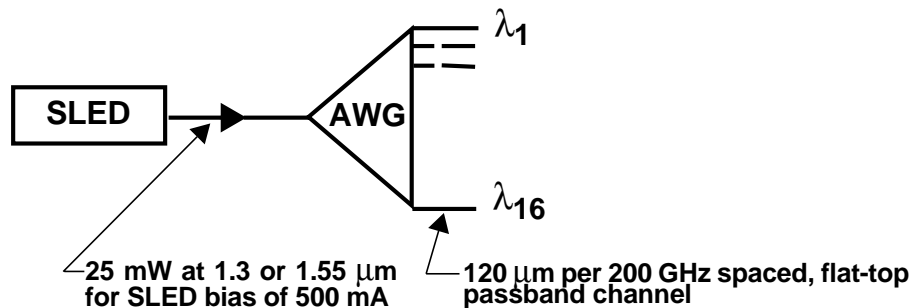
Optical transmission and performance characteristics of flat-top passband 16 channel/200 GHz channel spacing silica-on-silicon wavelength division multiplex filter.

Spectrally Sliced Amplified Spontaneous Emission Source

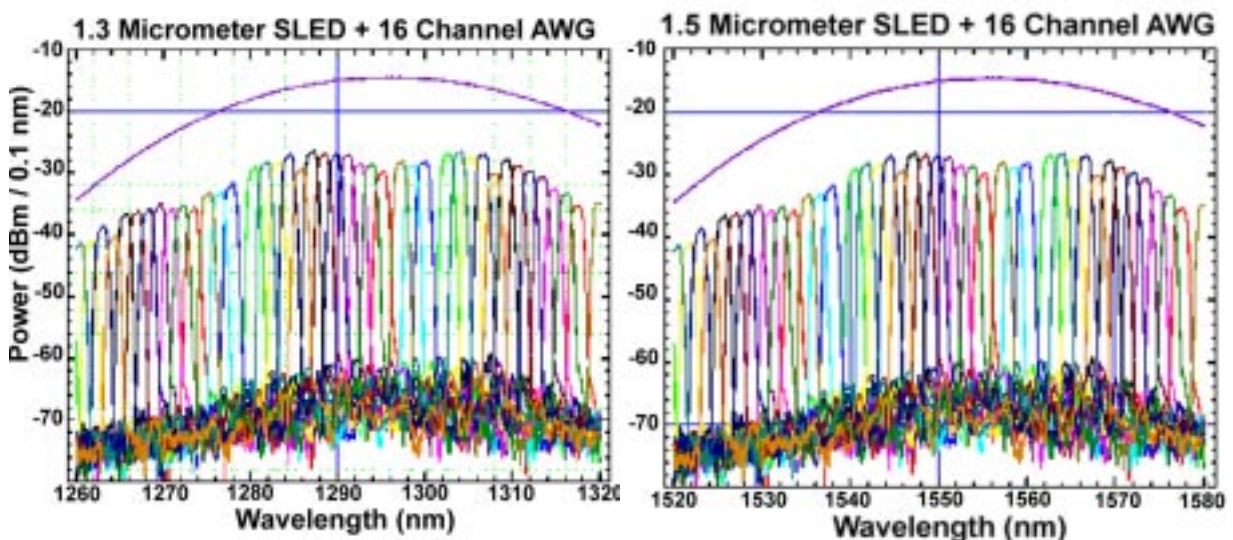
C. Holtmann*, E. Wildermuth, and H. Melchior

The combination of superluminescent light emission diodes (SLED's) with arrayed waveguide grating (AWG) filters leads to an amplified spontaneous emission (ASE) light source with geometrically separated wavelength-channels that is of interest for optical communications, sensors and metrology.

For such a multiwavelength source we combined the newly developed superluminescent LED's of Opto Speed for the 1.3 and 1.5 wavelength ranges that are capable of delivering up to 25 mW into 10 micrometer core single mode fibers with our 16 channel flat-top passband AWG-filters. Despite overall insertion losses of the AWG of 8 dB, up to 120 microwatts of light emerge from each of the sixteen geometrically separated 200 GHz spaced wavelength channels.



Superluminescent diode (SLED) driven sixteen wavelength channel arrayed waveguide grating (AWG) source.



Spectrally sliced amplified spontaneous emission source combining superradiant LED's with 16 channel, flat-top-passband AWG-filters (SLED and AWG spectra are shown).

* Opto Speed SA, Mezzovico

Polarization Insensitive Arrayed Waveguide Grating Filters in Indium Phosphide Applying Birefringence Compensation Scheme

M. Lanker

Arrayed waveguide grating filters are key components for wavelength channel multiplexing and demultiplexing in wavelength division multiplexed fiber optical communication systems. We realized such filters in the InP / InGaAsP material system which results in compact devices that offer the potential for integration with active optical elements, i.e. amplifiers, photodetectors as well as electronics.

The response of arrayed waveguide gratings depends on the refractive index of the base waveguides. Since these waveguides are in general birefringent, i.e. their effective refractive index is different for TE and TM polarization, the response of such filters is polarization dependent. This is unwanted for optical telecommunications.

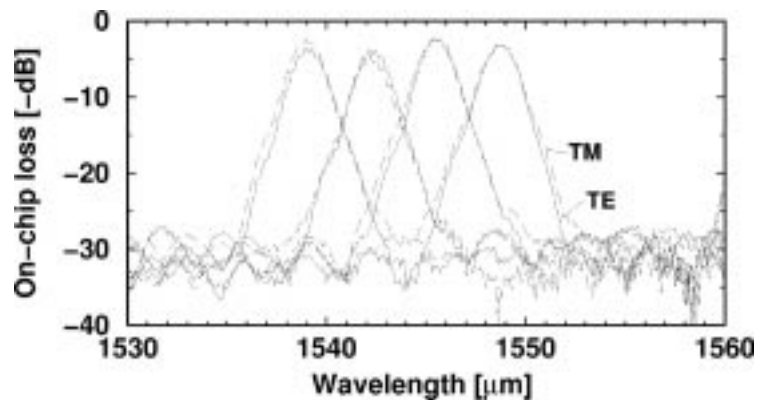
To obtain polarization insensitive devices, we applied a polarization dispersion compensation scheme to our phased arrays. This is done by inserting a modified waveguide section in each waveguide grating arm. The modified waveguide has a birefringence B' different to the one of the standard waveguide, B . Furthermore, the length of the modified section between one arm and its neighbor is increased by a constant value. The polarization dependent peak wavelength shift of such a filter is proportional to

$$\Delta\lambda \sim ((1-x)B + xB')$$

where x is the ratio between the length increase of the standard wavelength and the one of the modified waveguide. It is chosen by design for $\Delta\lambda = 0$.

Modification of the waveguide structure is done by varying the core width. Polarization insensitive phased arrays have been fabricated on InP substrate exploiting a buried waveguide structure. Measured results are shown in here.

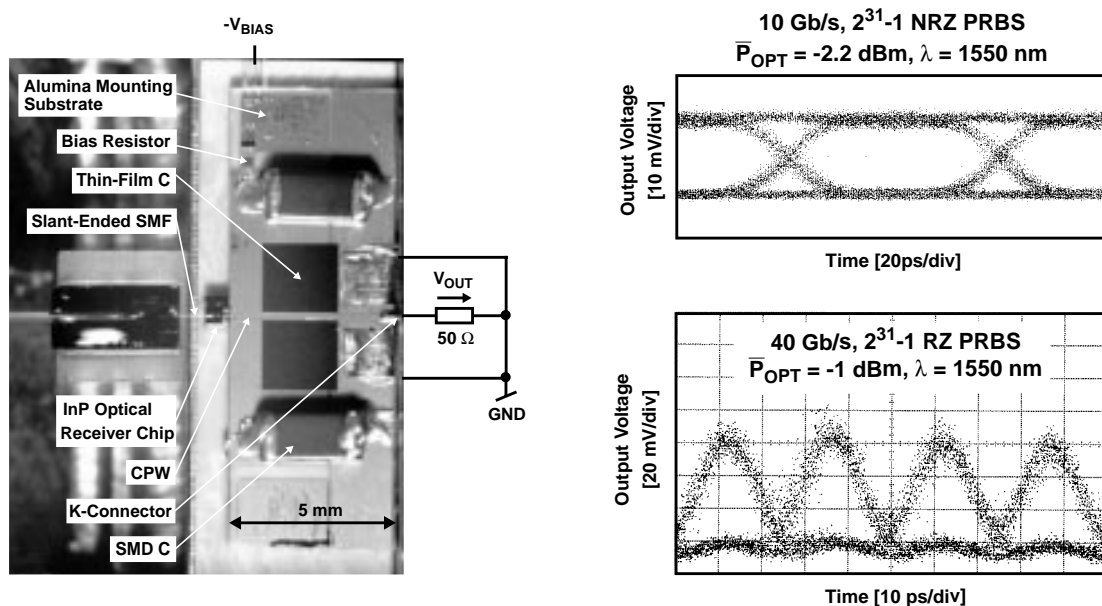
Transmission of an arrayed waveguide grating filter with 4 channels showing polarization insensitive operation. The device was implemented in the InP/InGaAsP material system.



Monolithic InGaAs/InP pin/HBT Optical Receiver Front-End Module for Datarates up to 40-Gb/s

M. Bitter, R. Bauknecht and W. Hunziker

Future time-division multiplexed (TDM) fiber-optic transmission systems with datarates up to 40 Gb/s require high-speed baseband optical receivers to detect and convert the incoming optical signals. The monolithic integration of such optical receivers offers the advantages of high-speed performance, reproducibility, small size and possible cost reduction of packaging. For the realization of our optical receiver chip we developed a fabrication technology to monolithically integrate top-illuminated pin photodiodes with single-heterojunction bipolar transistors (HBT) in the III-V InGaAs/InP material system. The optical receiver chip consists of a pin photodiode attached to a broadband darlington feedback amplifier circuit. To assembly the fully packaged module, the receiver chip is connected to an alumina mounting substrate by wire bonding. Both are incorporated in a brass housing featuring a slant-ended single-mode fiber to couple the incoming light into the top-illuminated pin photodiode and connectors for the DC power supply and the RF output signal. Our optical receiver module achieved an overall conversion gain of 48 V/W, an optoelectronic small-signal bandwidth of 30 GHz and clearly opened eyes for transmission experiments at 10 and 40 Gb/s, respectively.



Top-view photograph of optical receiver front-end module (left) and measured eye diagrams obtained from transmission experiments at 10 Gb/s and 40 Gb/s, respectively.

High-Current Indium Phosphide Double Heterostructure Bipolar Transistor Driver Circuits for Laser Diodes

H. Schneibel, R. Bauknecht, and C. Graf

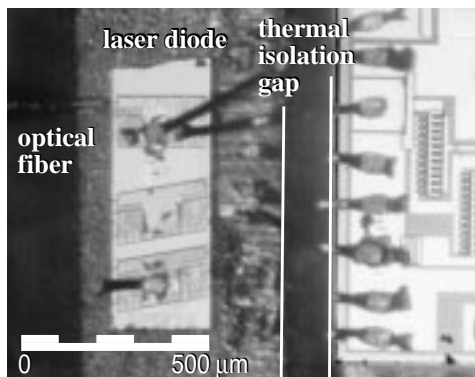
Electronic laser diode driver circuits are key elements in fiber optical communication networks. They provide enough current to operate a laser diode and also control the biasing condition of the diode to ensure fastest possible operation speed.

Today's general electronic equipment processes information which is represented as electrical voltage levels. To exchange information between devices separated through a long distance, optical pulses are much better suited than electrical pulses. Driver circuits convert electrical signals to currents qualified for driving laser diodes which therefore transmit optical signals corresponding to the electrical ones.

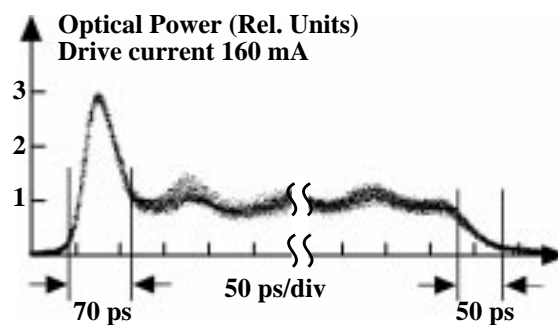
A current switch consisting of large multifinger heterostructure bipolar transistors builds the output stage that is designed to drive 200 mA into a laser diode load at frequencies up to 8 Gbit/s. Standard high speed ECL signals can be used to control this driver circuit. Input pins of the circuit are terminated to signal ground with on-chip 50 ohm resistors to match the impedance of signal sources and electrical wires. To cope with power dissipation at high driving currents, the dye is thinned to 120 μm and soldered onto copper heat sink to guarantee adequate cooling.

Best performance is achieved with a laser diode located next to the driver circuit. A thermal isolation gap between the driver circuit and laser keeps the diode thermally independent. Contrary to the passive cooling of the driver through a copper heat sink and housing, the laser diode is cooled actively with a peltier element.

For the optical measurements a pattern generator with 45 ps rise- and falltime was used as signal source for the driver circuit. A high speed photo diode with bandwidth of 40 GHz was connected to a 50 GHz sampling oscilloscope analyzing the optical pulse. The resulting rise- and falltimes of the optical pulse remain below 70 ps including laser relaxation effects.



Close up photograph of driver connected to a laser diode.



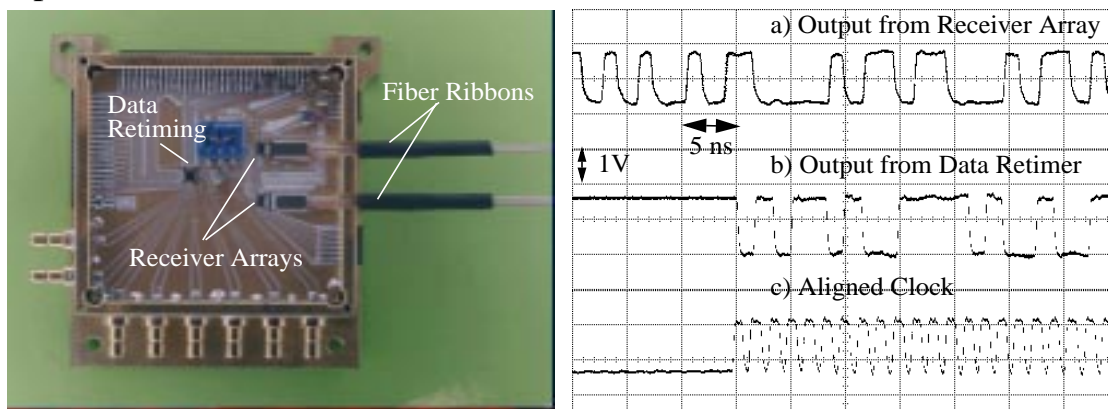
Optical response of laser diode directly driven by InP HBT driver with 160 mA modulation current.

Fiber Optical Burst-Mode Packet Receivers Operating at 155 Mbit/s and 622 Mbit/s

M. Bossard, C. Graf

In fiber optical networks receiver electronics often has to be capable of recovering traffic cells from a large number of different sources. Quick adaption to the different signal amplitudes and phases of consecutive incoming traffic cells is required. A Burst-Mode Receiver Module was designed and realized in CMOS technology that is capable of receiving 16 optical input channels at bit rates of 155 and 622 MBit/s. Long traffic cells with up to 10'000 bits and signal dynamics of 10 dB's can be selected rapidly within less than one microsecond.

The actual implementation of Burst-Mode Receiver Module combines InGaAs/InP photodetector wire bonded to custom-made silicon (CMOS) receiver electron-



Top View of 16:1 Burst Mode Receiver Module and Data Retimer

Digital 622 Mbit/s receiver array output, showing a) amplitude equalized outputs b) re-generated data, c) aligned clock

ics divided into three chips on an alumina MCM carrier substrate.

Two identical silicon chips feature two 8-channel receiver arrays including preamplifiers, peak-detectors, quantizers and channel selectors. The quantizers set the outputs to high in case the input signals exceed a threshold value, otherwise the outputs remain low. The threshold values are calculated internally for each individual traffic cell using peak-detection. This allows cell to cell optical input power variations of up to 10 dB.

The third chip contains a Data Retimer circuit. The circuit evaluates an appropriate phase of a plesiochronous clock reference for sampling the selected data channel. A PLL produces seven equidistant phases of the reference clock. The optimal clock phase is chosen by comparing samples, produced for all clock phases of the first few cell bits to an expected bit pattern. The optimal clock phase is then in the middle of the first and last hit. Further a validator/demultiplexer serves for word alignment and provides a decomposition of the data stream into 8 bit words.

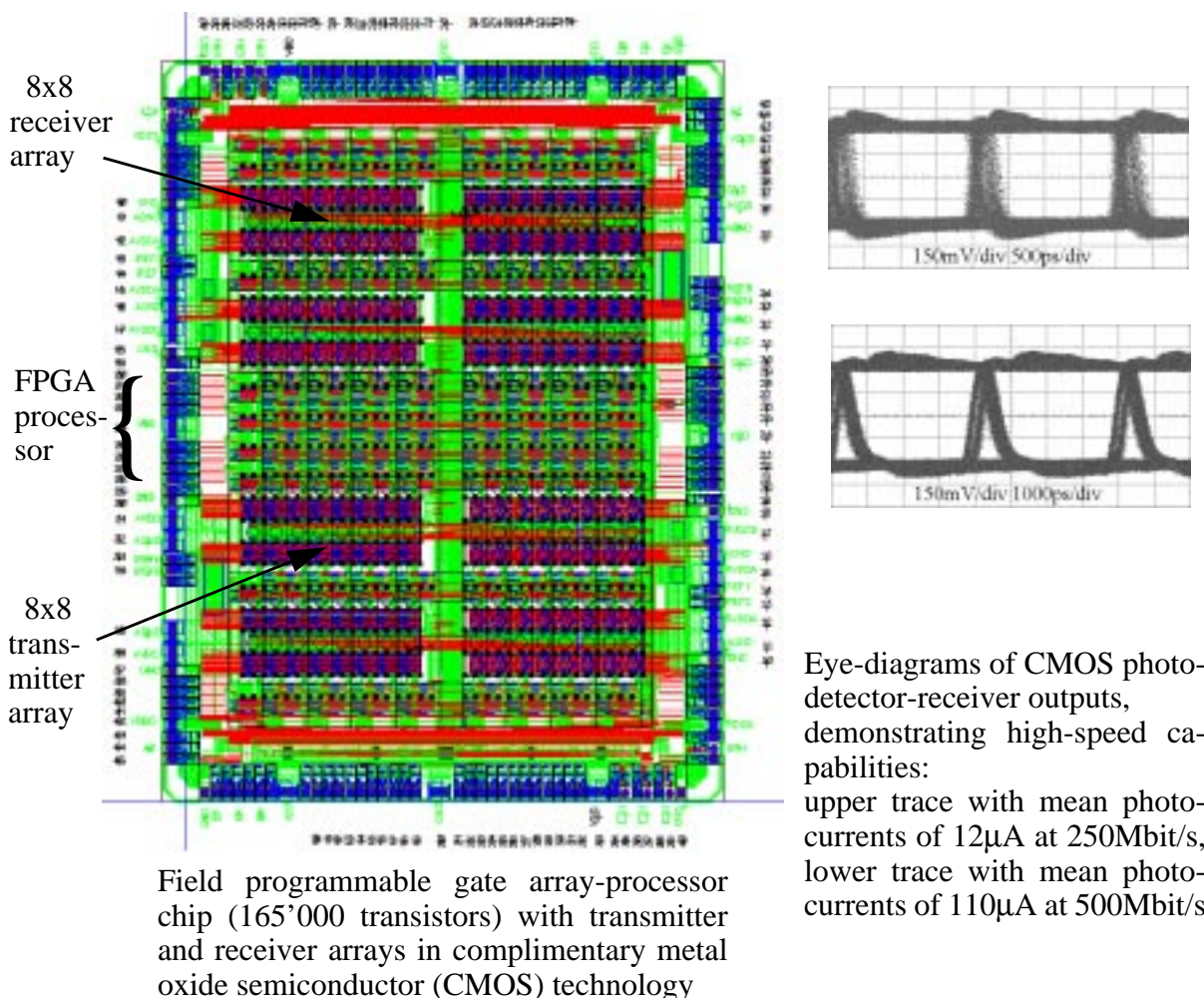
Complimentary Metal-Oxide Semiconductor Electronics for Processor to Processor Optical Interconnects

P. Zenklusen, R. Annen, H. Melchior

Massively parallel optical interconnects combining hybrid mounted light sources (vertical cavity surface emitting lasers, VCSEL's), plastic optical fibers and photo-detector arrays on digital CMOS-VLSI electronic circuits with monolithically built-in laser transmitters and photodetector-receivers are of interest for board-to-board communication.

In the frame of a European Research Project, a VLSI to VLSI optical interconnect is being demonstrated, that provides especially designed Field Programmable Gate Arrays(FPGA)-processors with four 8x8 optical links that are capable of data rates of up to 160 Mbit/s per link.

Our group designed the 8x8 CMOS transmitter and receiver electronics that was integrated into the digital FPGA-processor. Realized in a 0.6 micron gate-length CMOS technology, the VLSI-chips are currently being assembled with their opto-electronic and optics parts for the demonstration of an optical VLSI-processor to processor interconnect with a communication capacity of up to 256 x 160 Mbit/s.



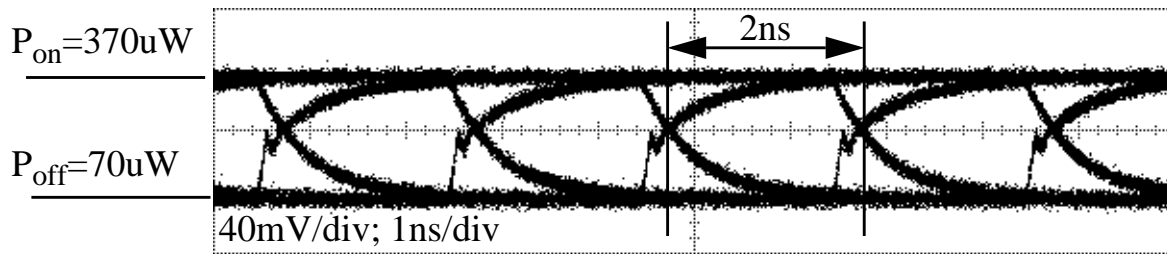
CMOS Laser Drivers for 4 Gbit/s Optical Interconnects

Richard Annen

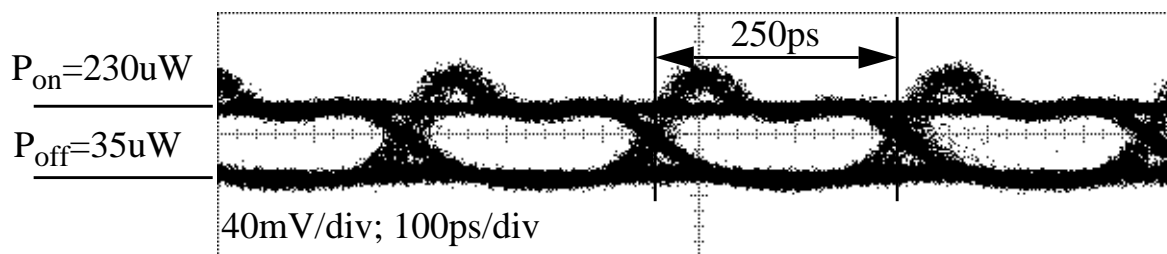
Optical links employing vertical-cavity-surface-emitting-lasers (VCSEL) are a promising alternative to electrical links for inter- and intra-board communication. In particular the low threshold current and low size of these devices make the realization of power efficient, high density parallel optical transmitters feasible. NxN multi-dimensional laser arrays are flip-chip mounted on CMOS VLSI chips which have appropriate I/O ports with CMOS laser driver circuits.

However the inherent high series resistance of low threshold VCSEL's may limit the modulation speed to less than 1 Gbit/s if conventional driver techniques are used. Therefore we developed driver circuits in 0.25 μm CMOS technology with optional current peaking operation mode to pre-compensate potential laser bandwidths limitations and thereby allow operation to higher bit rates.

A VCSEL driver realized in 0.25 μm CMOS technology, when operated in non-current peaking mode, allows VCSEL's with 270 Ohm series resistance to be driven up to bit rates of 500 Mbit/s. The same driver operated in peaking mode allows the same VCSEL to be driven up to much higher bitrates of 4 Gbit/s.



Optical output of 850 nm VCSEL with CMOS driver operating in non-peaking mode. Open eye diagrams show speeds extends to 500 Mbit/s.



Optical output of 850 nm VCSEL with CMOS driver operating in current peaking mode. Clear open eyes are maintained up to bit rates exceeding 4 Gbit/s.

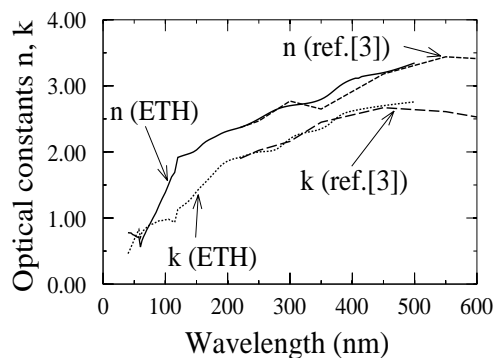
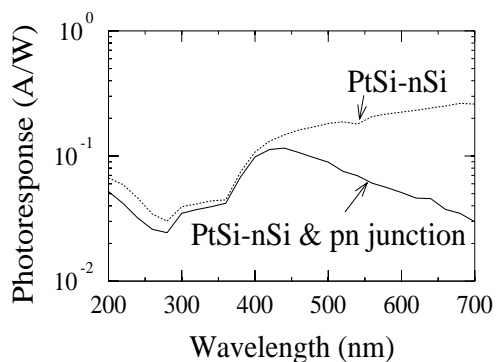
Large Area Solar-blind PtSi-nSi Photodetectors

K. Solt, and H. Melchior (ETH-Z, IQE, Micro- and Optoelectronics),
H. Henneken, P. Kuschnerus, H. Rabus, F. Scholze M. Richter
(Physikalisch-Technische Bundesanstalt Berlin)

A new kind of solar-blind photodetector has been developed, that combines the high stability and sensitivity in the UV with a suppressed photoresponse in the visible-near-infrared spectral ranges. The device is basically a PtSi-nSi photodiode that has an exceptionally large radiation hardness all along from the UV to soft X-ray range, as measured at the soft X-ray and UV/VUV detector calibration facilities of the Physikalisch-Technische Bundesanstalt in Berlin [1], containing, however, an additional, sub-surface potential barrier, that prevents collection of charge carriers created at depths below this barrier.

The advantage of this structure over the traditional junction diodes is its radiation hardness, due to the lack of protective oxide on the light-sensitive surface. Moreover, the light-sensitive area of the diodes is not limited by any technological factor, it can be as large as those of the common silicon Schottky diodes, which is their great advantage over the GaN and other compound-semiconductor solar-blind diodes.

New achievement is, that for the first time, the optical constants n and k of thin PtSi layers for wavelengths of $\lambda < 200$ nm have been experimentally determined [2].



Spectral responsivity vs wavelength for a solar blind PtSi-n-Si Schottky photodiode, containing an additional p-n junction (lower curve), and for the same PtSi-n-Si Schottky structure without any additional pn junction (upper curve).

Refractive index n , and extinction coefficient k determined on our thin PtSi films in the wavelength range of 50 to 500 nm. As a comparison, the n and k values of a 20 Angstrom thick PtSi film above $\lambda=200$ nm [3] are also shown.

[1] H. Rabus, V. Persch and G. Ulm, *Appl. Optics* **36** (1997) 5421-5440

[2] P. Kuschnerus, "Quantenausbeute von kristallinem Silizium im Spektralbereich von 40 nm bis 400 nm.", Dissertation der Technischen Universität Berlin, D83, 1999.

[3] C.K. Chen, B. Nechay, and B-Y. Tsaur, *IEEE Trans. Elect. Dev.* **38**, 1094, 1991

New insights into low dimensional structures and wafer fused devices

A. Rudra, F. Lelarge, K. Leifer, E. Kapon, E. Gini, M. Ebnoether

This is a selection of results obtained through the collaboration with the nanostructure group of Prof. Kapon in EPFL.

Quantum wires and microcavities

(C. Constantin, E. Martinet, B. Gayral, J.M. Gérard)

Dense arrays of $\sim 10\text{nm}$ size, strained InGaAs/GaAs V-groove quantum wires (QWRs) were incorporated in a wavelength-size planar Bragg microcavity using several growth steps. Ridge- and pillar-like microresonators were then processed from the planar cavity using lithography and etching techniques, in order to provide the lateral photon confinement in photon wires and boxes. Resonant coupling between the wires and a planar microcavity results in a strong reduction of the photoluminescence linewidth (~ 10), and a significant increase of the on-axis intensity ($\sim \times 50$) of the InGaAs QWRs. When the planar microcavity is etched into a 4mm -wide pillar, the coupling with the resonant modes of the photon box leads to a series of extremely narrow (0.45meV) PL emission peaks.

Wafer-fused VCSEL's and resonant photodetectors at $1.5\ \mu\text{m}$

(A. Sirbu, V. Iakovlev)

8×1 VCSEL arrays with emission wavelengths regularly spaced between 1520nm and 1530nm were obtained by adjusting the cavity length before the wafer fusion process. Anodic oxidation was used to adjust the height of the mesas used in the localized fusion process to correspond to each laser of the array.

Single mode emission with a side mode suppression in excess of $40\ \text{dB}$ is obtained under optical pumping.

VCSEL structures were also evaluated as resonant photodetectors and showed a detection spectrum with a FWHM as narrow as 0.02nm at 1527nm under forward bias.

Few-particle states in the optical spectra of single quantum dots

(A. Hartmann, Y. Ducommun, D. Oberli)

The number of excess electrons in pyramidal shaped quantum dots (QDs) was controlled using above barrier laser excitation. In the micro-photoluminescence spectra, we identify transitions corresponding to the recombination of neutral and up to 5 times charged single- and multi-excitons.

Optical processes in AlGaAs/GaAs V-groove quantum wire waveguides, diodes and LEDs (E. Martinet, H.Weman, M.A. Dupertuis, L. Sirigu)

- Electron injection was shown to be the most effective mechanism for altering the QWR absorption. We observed a complete quenching of the absorption edge in n-Schottky diodes with a Burstein-Moss blue shift associated with the filling of several electron subbands. An electro-optic modulator was hence realized using a single-QWR p-i-n diode embedded in a V-shaped dielectric waveguide. The room temperature absorption edge was red-shifted by more than 40nm under electron injection.

- Efficient selective carrier injection through the vertical quantum well results in narrow linewidth electroluminescence at room temperature. Injection experiments into asymmetric double QWRs under high magnetic field indicate that emission originates from strongly Coulomb-correlated 1D excitons up to very high carrier densities.

In segregation in InGaAs/GaAs quantum wires (F. Lelarge, K. Leifer, C. Constantin)

Electron Energy Loss Spectroscopy allowed the quantitative mapping of the In content in InGaAs QWRs. A strong segregation develops at the bottom of the wire due to the larger diffusion length of the In containing species. This segregation produces a vertical quantum well structure with a few nanometers wide central branch showing an InAs content up to 30% for a nominal value of 15%. An intense room temperature PL emission with a linewidth as narrow as 30meV was obtained from dense ($4/\mu\text{m}$) InGaAs QWR arrays at a wavelength of 1.16 μm .

Direct observation of quantum contact resistance (D. Kaufmann, B. Dwir, I. Utke, A. Palevski)

In modulation doped GaAs/AlGaAs QWR structures, the electrons access the QWRs non-adiabatically through a 2D-1D transition zone. Each level of quantized conductance is therefore reduced by a quantum contact resistance. This resistance was measured as a function of the transition zone length through electrostatic control. It was shown that below a critical contact length, 2D-1D electron transition can be totally inhibited due to insufficient 1D-2D coupling.

Opto Speed SA

R. Dall'Ara, M. Blaser, W. Hunziker, Ch. Holtmann, J. Eckner, R. Bauknecht and coworkers

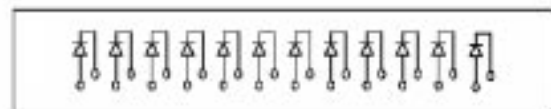
Opto Speed SA is a Spin-off company of the Micro- & Optoelectronics Laboratory of the Institute of Quantum Electronics. It has been founded in 1995 to exploit some of the excellent research work by specific product developments. Based on the fabrication of chips and modules for the tele- & datacom market realized in InP based semiconductor technology the company has expanded to 15 employees. Main product areas are photodetectors, semiconductor optical amplifiers (SOA's) and super luminescent light emitting diodes (SLED's), as well as the hetero bipolar transistor (HPT) technology for integrated optoelectronic devices such as receivers. The following parts gives some examples of the photodetector, SLED, and HPT area.

InGaAs/InP Photodetectors

The photodetector technology is based on pin photodiodes in InGaAs on InP semi insulating substrates grown by MOVPE. A large variety of different types of photodiodes for different applications in telecom, datacom and metrology have been realized. Photodiode diameters vary from more than 100 μm for tolerant coupling to multi mode fibers down to 12 μm for very high speed applications. Different designs also include single photodiodes or arrays where the pitch between the photodiodes for parallel interconnect is kept to 250 μm to allow direct coupling to ribbon fiber cables. Further variations are top- and back illuminated devices for different applications and packaging technologies. For the back illuminated devices the sensitive wavelength range is limited from 980 to 1600 nm as the shorter wavelengths between 800 and 980 nm are absorbed by the InP substrate.



Photograph of photodiode chip with \varnothing 32 μm diode and electrical coplanar transmission lines for high speed applications

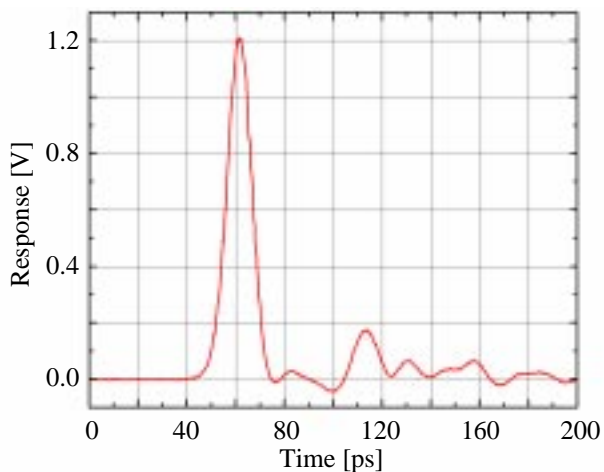


Layout and photograph of 12 channel photodiode array chip with 250 μm pitch between photodiodes to allow direct optical coupling to fiber ribbon cable

Another strong feature of the photodiode structure is the full depletion of space charge region at voltages below 2.5V. The full speed of response can therefore be achieved in connection with standard high speed electronic IC's. High speed photodetector modules for telecom applications and metrology up to 40 GHz are realized by packaging of high speed photodiodes with bias-T and optical coupling to single-mode fibers.



High speed photodetector module for applications up to 40 GHz with single mode fiber pigtail and integrated bias-T



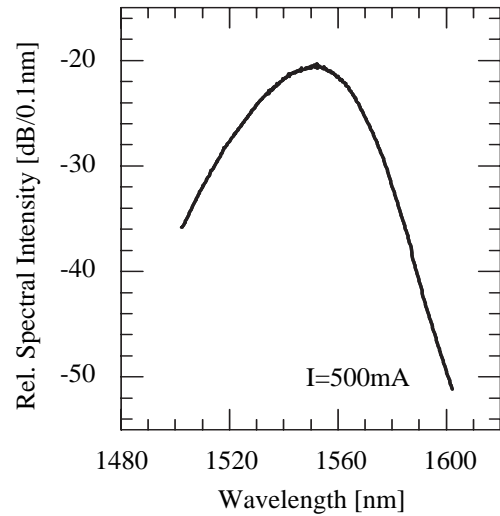
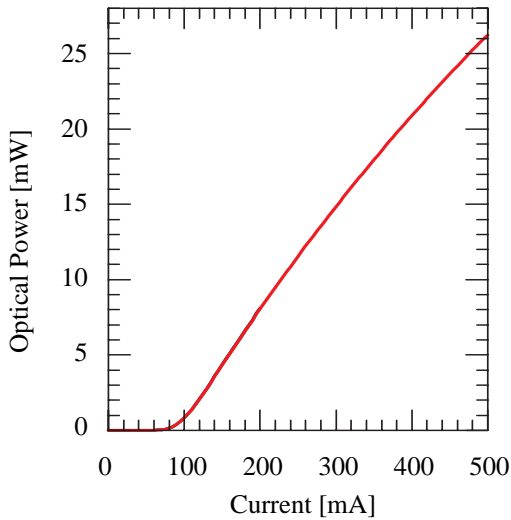
Impulse response of high speed photodetector module showing FWHM < 12 ps

Super Luminescent Light Emitting Diodes

Super luminescent light emitting diodes (SLED's) are of great interest for optical low coherence reflectometry, spectrum-sliced wavelength division multiplexed systems, fiber-optic sensors and optical waveguide characterization. Opto Speed produces SLED's packaged in DIL housings that can offer ultra high output powers of more than 20mW in a single-mode fiber, low spectral ripple of less than 0.1dB or bandwidths of more than 60nm at FWHM. These compact SLED's are available for the wavelength ranges around 1310nm, 1400nm as well as for 1550nm. New SLED's are developed for the extended wavelength range around 1620nm. The fabrication of edge-emitting super luminescent light emitting diodes is based on InGaAsP / InP material system and exploits the ridge-waveguide structure with bulk or multiple quantum well active region.



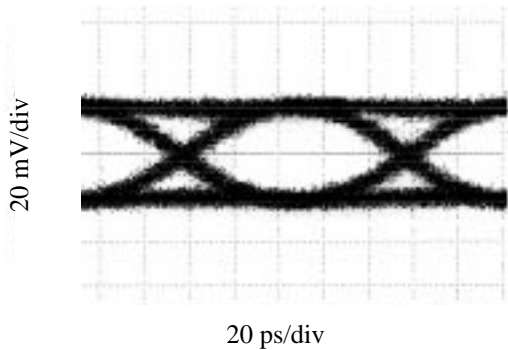
SLED in 14 pin DIL package with single mode fiber pigtail



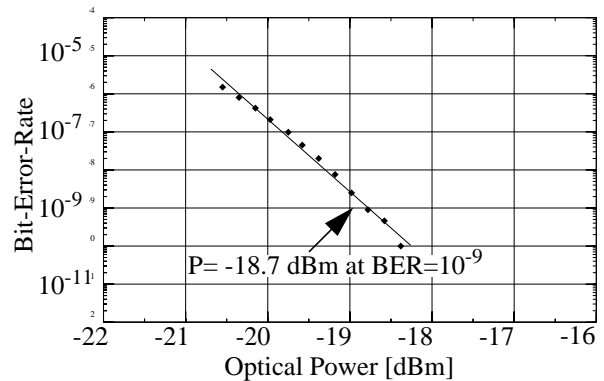
Module output power in single mode fiber and corresponding emission spectrum of ultra high power SLED module emitting around 1550 nm

High-Speed Optical Receivers

Opto Speed's high-speed fiber-optical receivers are designed for 10 Gb/s OC-192/STM-64 SONET/SDH high-capacity fiber-optical communication networks. The advanced technological concept of these devices is based on the monolithic integration of InP-HBT (hetero bipolar transistor) preamplifiers and InGaAs-pin-photodiodes, which offer both exceptional performance and low power consumption.



Eye diagram at 10 Gb/s
 $2^{31}-1$ PRBS NRZ
 Wavelength 1.55 μm
 -15 dBm optical power



Bit-error-rate measurement at
 10 Gb/s $2^{31}-1$ PRBS NRZ
 Wavelength 1.55 μm

References: Datasheets at www.optospeed.ch

Development of Superstrate Cu(In,Ga)Se₂ Solar Cells

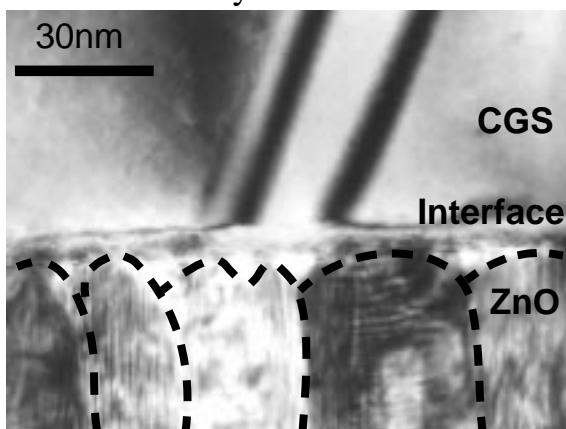
F. -J. Haug, M. Krejci, H. Zogg, A.N. Tiwari

Thin film solar cells are grown in a “substrate” or “superstrate” configuration. We have grown ZnO:Al/ZnO/CdS/Cu(In,Ga)_xSe_y/Mo/glass substrate solar cells with an efficiency of 15.7%. In this case a transparent encapsulation material as well as another glass cover are required. In the superstrate solar cells the supporting glass simultaneously is used as encapsulation. In this configuration the p-type CIGS absorber layer is grown on a wide band-gap n-type semiconductor which acts as a front contact also. The chemical and electrical stability of the front contact is important as process temperatures of about 500°C during the absorber deposition may cause interdiffusion and thus influence the electronic characteristics of the junction.

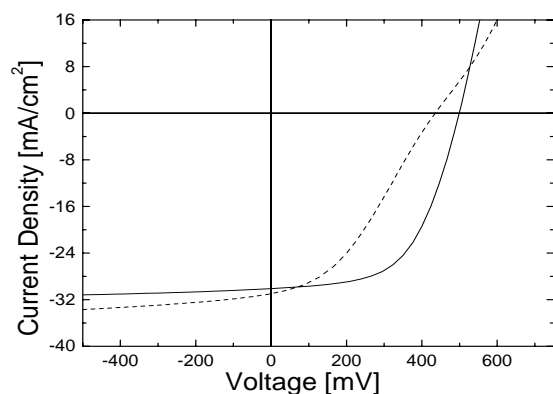
Superstrate solar cells are fabricated on glass coated with a bilayer of intrinsic and Aluminum doped ZnO. These layers are grown by RF magnetron sputtering. The CdS buffer layer which has a beneficial effect in the case of substrate solar cells can not be used in this configuration due to strong interdiffusion during the vacuum deposition of the absorber-layer.

Transmission Electron Microscopy (TEM) has been used to investigate the microstructure of the interface between ZnO and CIGS and an interfacial layer of 5 nm thickness has been found. Additionally a high content of Gallium was found in the interfacial region. The migration of Gallium toward the interface causes a non optimal doping profile across the junction. This could explain the observation of a double diode in the I-V-characteristic of Au/CIGS/ZnO/ZnO:Al/glass superstrate solar cells.

Improvements in the diode characteristics are obtained when the CIGS absorber layer is grown with a Gallium depleted initial stage. Thus superstrate solar cells with an efficiency of 8.5% have been fabricated.



TEM Cross Section of the interface between CuGa_xSe_y and the ZnO layer. The formation of an interfacial layer is observed.



The double diode in the I-V-characteristic is avoided by a Ga-depleted start of the growth.

Sponsor: BBW/EU (JOULE project)

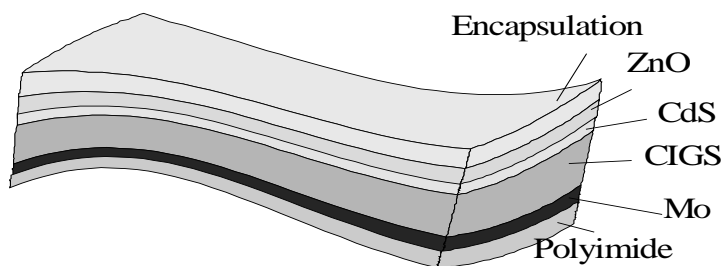
Lightweight and Flexible Cu(In,Ga)Se₂ Solar Cells on Polymer with a World Record Efficiency of 12.8%

M. Krejci, D. Rudmann, F.-J. Haug, H. Zogg, A.N. Tiwari

Development of high efficiency, stable, lightweight and flexible solar cells is important for novel terrestrial applications. The Cu(In,Ga)Se₂ (CIGS) solar cells are also promising for space applications because their stability against high energy irradiation are superior to crystalline Si and GaAs solar cells. The CIGS cells on polymers can yield a very high specific power of about 1.5 kW/kg, which is 3-4 times higher than that of conventional Si solar cells.

Typical CIGS absorber layers for high efficiency solar cells are grown on Mo coated soda-lime glass substrates at temperatures of about 550°C. A certain amount of Na and high deposition temperatures are required for an optimum carrier concentration and morphology of the CIGS absorber layer. None of the known polymers can withstand such high temperatures and they do not contain Na. Thus low efficiency solar cells are expected on polymers.

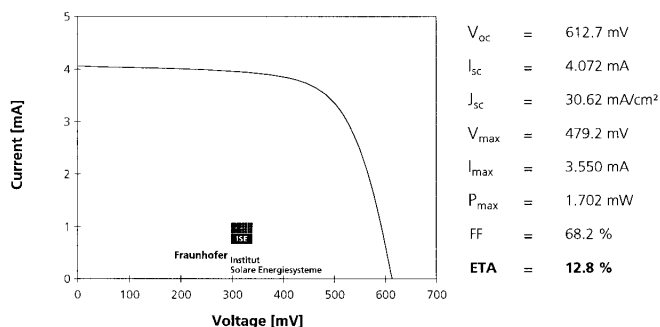
A lift-off process has been developed to obtain CIGS solar cells on polymer films. The absorber layer is grown by a co-evaporation method on a polyimide layer, which is spin coated on a NaCl covered glass substrate. The NaCl intermediate layer can provide Na to the CIGS layer during deposition. After the complete processing of the cells, the NaCl buffer layer is dissolved to separate the glass substrate from the ZnO/CdS/CIGS/Mo/polyimide stack. The total thickness of the solar cell including polymer substrate is less than 25 microns. A record conversion efficiency of 12.8% was independently measured at FhG/ISE, Freiburg, Germany. This is the highest reported efficiency for any type of solar cell grown on polymers.



Schematic diagram of the ZnO/CdS/CIGS/Mo/polyimide flexible solar cell.

I-V Record AM 1.5 global, 1000 W/m², 25° C **Date:** 15.06.99

Identification: FL14-I/C4 **Manufacturer:** Inst. Quantum Electr. ETHZ **Customer:** Inst. Quantum Electr. ETH



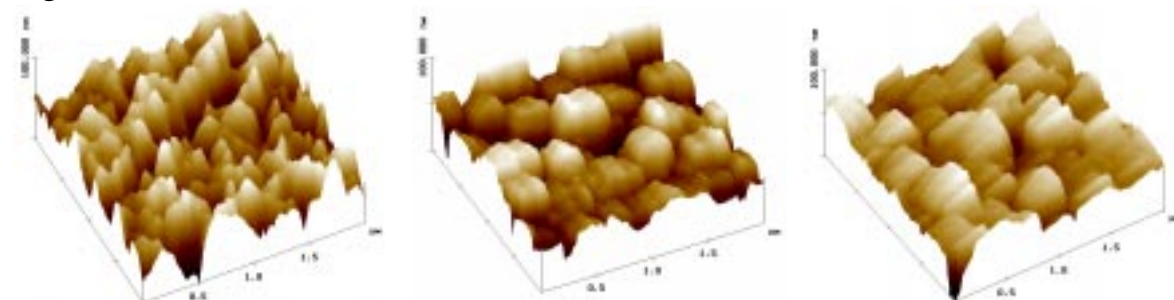
I-V characteristic of a 12.8% efficiency CIGS solar cell on polyimide layer measured under AM1.5 illumination.

Sponsor: BBW/EU (JOULE project)

CdTe/CdS Thin film Solar Cells

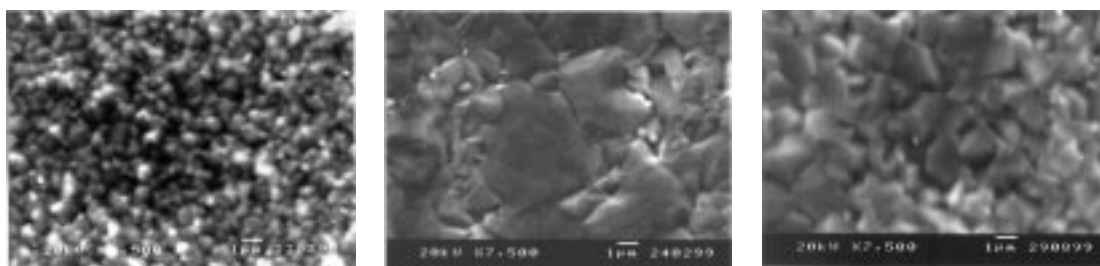
A.Romeo, D.L. Bätzner, H.Zogg, A.N. Tiwari

CdTe/CdS solar cells are grown by a high vacuum evaporation (HVE) method on glass substrates covered with a transparent conducting oxide (TCO). The morphology of CdS layers and its conformal coverage of the TCO substrate depends on the deposition process and post deposition annealing treatment. The grain size of HVE-CdS is in the range of 0.1 to 0.3 μm and the layers are rough. If the CdS is grown by a chemical bath deposition (CBD) then it consists of small grains of about 0.1 μm width which coalesce together and form clusters of about 0.5 μm size. A treatment with CdCl_2 recrystallizes the CdS layers so that some of the small grains coalesce together and form bigger grains of 0.5 μm width. The grain size and crystallographic orientation of CdTe on different CdS layers have been investigated and correlated with the photovoltaic properties. As shown in bottom figure the grains of CdTe on HVE-CdS are in the range of 0.5 to 1 μm . The CdTe on CBD-CdS consists of some grains of about 1 μm and many grains of about 5 μm width. The grains of the CdTe on CdCl_2 treated HVE-CdS are in the intermediate size range.



Morphology of HVE-CdS (left), CBD-CdS (centre) and CdCl_2 treated HVE-CdS (right).

A “ CdCl_2 treatment” is performed for the recrystallization of CdTe and activation of the CdS-CdTe heterojunction. The cells with CBD-CdS exhibit low efficiency (5.6%) due to the presence of pinholes and excessive intermixing of CdS-CdTe at the interface. The efficiency of cells on CdCl_2 treated HVE-CdS is 11%, while the highest efficiency of 12.5% ($V_{\text{oc}}=800$ mV, $I_{\text{sc}}=23$ mA/cm², FF=0.67) is obtained for the cells on HVE-CdS.



Morphology of as-deposited CdTe on HVE-CdS (left), on vacuum annealed CBD-CdS (centre) and on CdCl_2 treated HVE-CdS (right).

Sponsor: BBW/EU (JOULE project)

Efficient and Stable Electrical Contacts on CdTe/CdS Solar Cells

D. Bätzner, A. Romeo, H. Zogg, A. N. Tiwari

The long term stability and efficiency of CdTe/CdS solar cells depend on the “CdTe back contacting” process. CdTe has a high electron affinity (above 5 eV), therefore a metal of high workfunction is required to form an ohmic contact on p-type CdTe. Most of the materials form a Schottky barrier with p-CdTe and restrict the solar cell efficiency. To obtain an Ohmic contact or quasi-ohmic tunneling contact a buffer layer between the CdTe and the metal is incorporated.

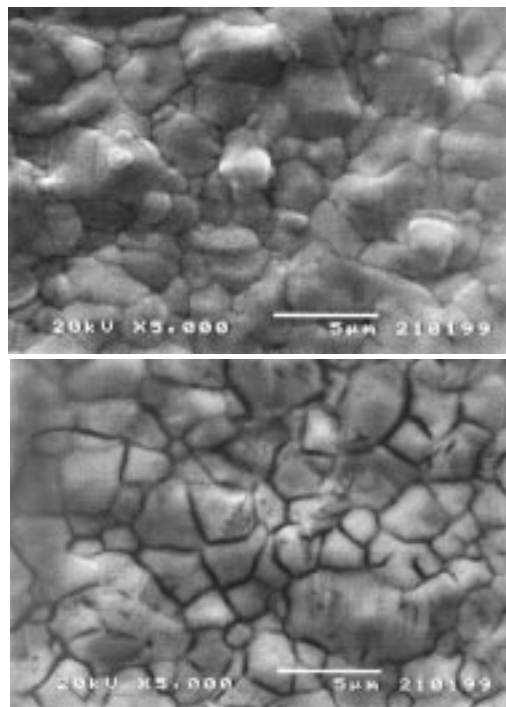
This buffer layer is of a degenerated semiconductor of high carrier concentration which reduces the Schottky barrier height.

Conventional back contacts on CdTe/CdS solar cells are commonly made with Cu/Au or Cu/graphite. Usually such contacts limit the solar cell efficiency and the performance degrades because of the Cu diffusion across the junction.

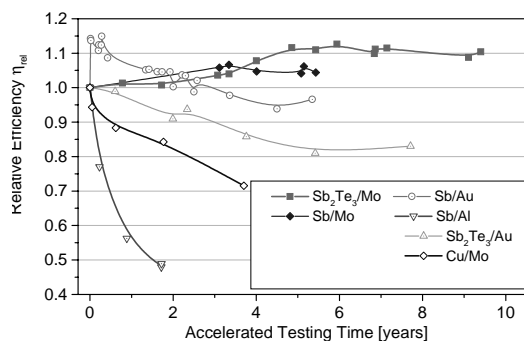
In order to develop “non-rectifying” and stable electrical contacts the CdTe surface was etched. Different etchants were investigated to clean the CdTe layer and produce a highly conductive Te-rich surface which increases the doping concentration of the back contact. First figure shows the morphology of CdTe etched with a mixture of nitric and phosphoric acid.

We have used vacuum evaporated Sb_2Te_3 and Sb buffer layers for the first time to obtain highly efficient and stable solar cells. Investigations have clearly shown that the long term stability depends on the metallization also. CdTe/CdS solar cells with efficiencies of 12.5% and stability of more than 10 years according to accelerated test conditions have been developed.

Sponsor: BBW/EU (JOULE project)



CdTe morphology before (top) and after (below) etching with nitric-phosphoric acid.



Long term stability of CdTe solar cells with different back contacts.

Heteroepitaxial high quality narrow gap lead-chalcogenides on Si(111) and formation of quantum dots

K. Alchalabi, H. Zogg

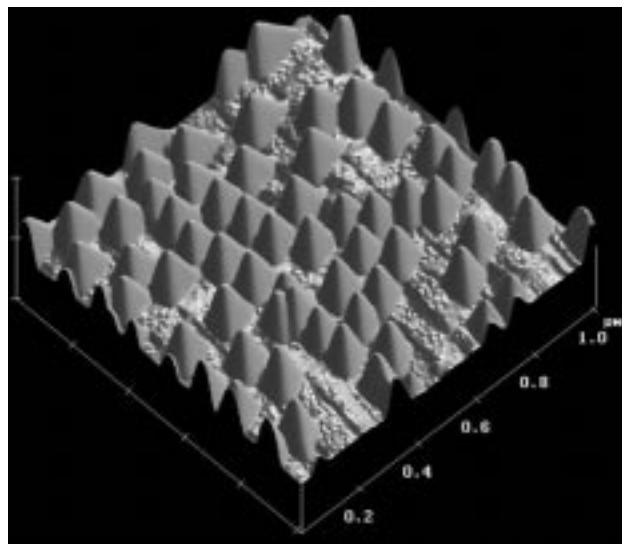
High quality epitaxial lead-chalcogenide layers like PbTe and PbSe are obtained on Si(111) substrates by molecular beam epitaxy. The large lattice mismatch as well as the thermal expansion mismatch lead to a high number of dislocation lines at and near the interface. Since dislocations are highly mobile in high quality lead-chalcogenides and due to the thermal mismatch, the threading ends of the misfit dislocations move on each temperature change in order to relieve the thermal mismatch strain. If two threading ends meet within a certain reaction distance, and if their Burgers vectors are appropriate, they react: They either annihilate, or fuse in a manner that one dislocation only is left. Therefore, the number of threading ends at the surface of the layer decreases on each temperature change. From the rate of the decrease, we calculated a reaction radius of about 7 nm.

For lead-chalcogenides, the low temperature saturation mobilities μ_{sat} are entirely determined by the dislocation densities (This is contrary to e.g. III-V semiconductors, where μ_{sat} is limited by impurity scattering).

The highest μ_{sat} reported for lead-chalcogenides are $\sim 3 \cdot 10^6 \text{ cm}^2/\text{Vsec}$ and correspond to dislocation densities below 10^6 cm^{-2} . For our epitaxial layers on extremely lattice-mismatched Si(111) substrates, the highest μ_{sat} are still 200'000 to 500'000 cm^2/Vsec , this corresponds to dislocation densities in the mid 10^6 cm^{-2} range.

Layers with such dislocation densities allow the fabrication of infrared devices as well as of well oriented quantum dots: If the PbTe layer is overgrown with a suitable amount of PbSe (lattice mismatch 5%), equally oriented dots with triangular side faces corresponding to (100) planes form with near uniform sizes. Such dots are of interest for optoelectronic applications like quantum dot emitters.

Sponsor: Swiss NF



AFM image of PbSe on PbTe(111) quantum dots. The side faces of the dots correspond to (100) planes.

Development steps of a 128 x 96 heteroepitaxial narrow gap infrared sensor array on a silicon read-out chip

K. Alchalabi, Q. Lai, H. Zogg, E. Gini

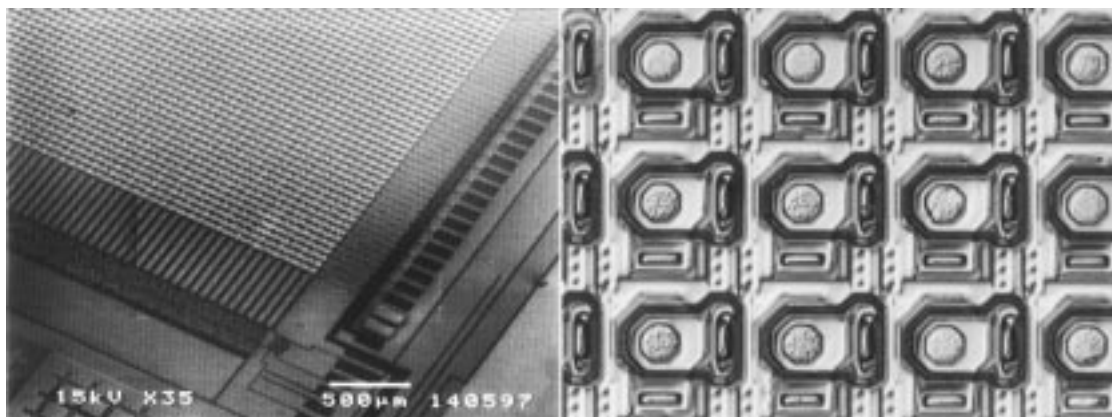
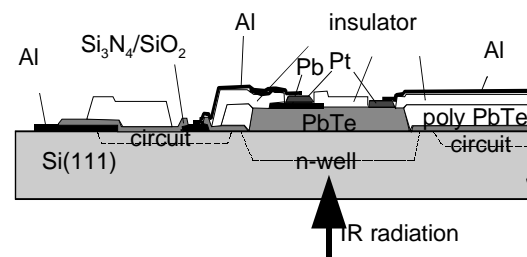
Narrow gap semiconductor (NGS) infrared sensors for thermal imaging exhibit the highest sensitivities at a given operating temperature. The signals of the individual pixels are read-out serially with a silicon multiplexer. Present systems with e.g. a large array of InSb or $\text{Hg}_x\text{Cd}_{1-x}\text{Te}$ IR-sensors are fabricated in a hybrid manner: The NGS sensor chip is mated to the Si read-out chip with indium bumps. The high number and small pitch of the In-bumps yields to an expensive technology. By growing the NGS IR-sensor layer directly onto the Si read-out chip, a considerable simplification results, and a wafer scale technology becomes possible. Such devices have not been realized up to now.

For our demonstration, we use lead-chalcogenides as NGS-material. These IV-VI semiconductors are considerably easier to handle, but exhibit the same ultimate sensitivities as e.g. $\text{Hg}_x\text{Cd}_{1-x}\text{Te}$. The read-out chips with 128 x 96 pixels on 75 μm pitch were fabricated in CMOS technology in Si(111). They contain individual addressing transistors for each pixel and a multiplexer.

Layers of PbTe with about 3 μm thickness are grown by molecular beam epitaxy onto the read-out chip. The temperature budget does not exceed 450°C for 1 h because of the Al-metallization. The PbTe-layer is etched to individual pixels and sensors are fabricated. The blocking Pb-contacts as well as the ohmic contacts and Al-fan-out are delineated by lift-off techniques. As insulator layer, a photosensitive polyimide is employed, and RIE serves for openings in the $\text{Si}_3\text{N}_4/\text{SiO}_2$ passivation layer of the read-out chip.

Presently, all these steps are developed, and a few arrays were successfully processed for the first time.

Schematic cross section, part of the 2-d array, and some individual pixels after complete processing.



Packaging of PbTe-on-Si infrared sensor arrays for thermal imaging

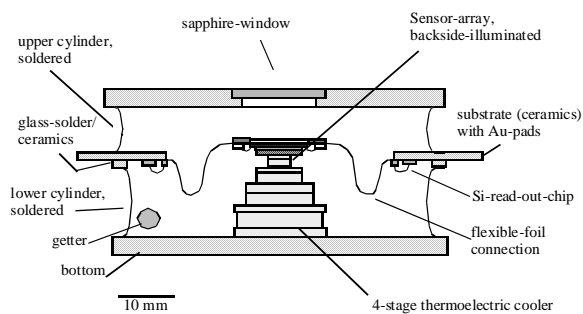
H. Zogg, K. Alchalabi, M. Leopold

A compact sealed package for a thermoelectrically cooled linear PbTe infrared sensor array sensitive in the 3-5 μ m wavelength range was designed and realized. The sensor array contains 128 pixels and is soldered onto a 4-stage thermoelectric cooler. The two read-out chips each containing 64 parallel low-noise integrators and one serial analog output are bonded on a ceramic substrate and operated at room temperature.

The electrical connections between the cooled sensor pixels and the inputs of the amplifiers are realized with a novel low thermal conductivity flexible kapton foil which contains thin film gold leads as conductors.

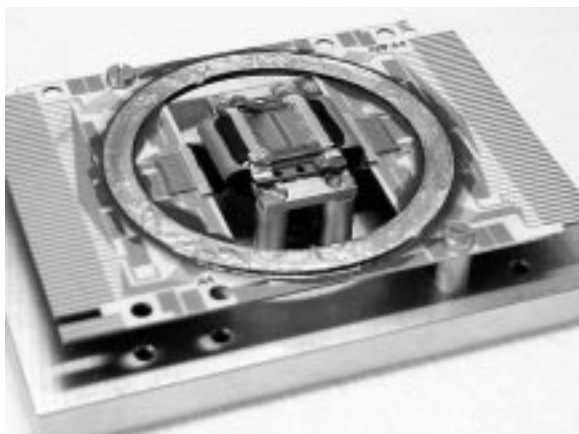
The electrical connections to the outside world are formed on the same ceramic substrate with the aid of novel planar thin-film feed-throughs. The pitch of the Au-pads serving as feed throughs is 250 μ m. For electrical insulation, a low temperature glass solder is used which solders the substrates containing the electric lines to a ceramic ring. The top of the package with a sapphire window as well as the bottom onto which the high temperature side of the thermoelectric cooler is soldered complete the package. The solderings have to be performed with different low temperature alloys since the thermoelectric coolers do not withstand temperatures higher than 138 $^{\circ}$ C.

A nonevaporable getter is used to maintain the vacuum. The sensor array and package are fully operative, a sensor temperature below -66 $^{\circ}$ C is reached.



Cross section (left), Ceramic substrate with IR-array and ribbon cables on test fixture (bottom left), completed package (bottom).

Sponsors: GRD, KTI



PUBLICATIONS 1999

Microelectronics and Optoelectronics Laboratory

Books, Book Chapters and Reviews

W. Hunziker

"Hybrid Integration and Packaging of InP-Based Optoelectronic Devices"
InP-Based Materials and Devices: Physics and Technology, Edited by O. Wada and
H. Hasegawa, Chapter 14, pp. 537 - 581, ISBN 0-471-18191-9, 1999

J. Leuthold

"Advanced Indium-Phosphide Waveguide Mach-Zehnder Interferometer All-Optical
Switches and Wavelength Converters"
Hartung-Gorre Verlag Konstanz, Series in Quantum Electronics, **12**, 303 pages,
ISBN 3-89649-427-9, 1999

H. Melchior and E. Gini

"Indium Phosphide and Related Materials (IPRM'99)"
Conference Proceedings, 588 pages, Post Deadline Papers, 31 pages, and Exhibition
Guide, 43 pages, IEEE Catalog No. 99CH36362, ISBN 0-7803-5562-8, 1999

Ch. Nadler

"Polarization Insensitive Arrayed Waveguide Grating Wavelength Multiplexers for
Optical Communication"
Hartung-Gorre Verlag Konstanz, Series in Quantum Electronics, **10**, 197 pages,
ISBN 3-89649-394-9, 1999

A. Schmid

"Receiver Arrays for Chip and Board Optical Interconnects"
Hartung-Gorre Verlag Konstanz, Series in Microelectronics, **79**, 149 pages,
ISBN 3-89649-424-4, 1999

Journal Publications (chronological)

Ch. Guillemot, M. Renaud, P. Gambini, Ch. Janz, I. Andonovic, **R. Bauknecht**, B. Bostica, M. Burzio, F. Callegati, M. Casoni, D. Chiaroni, F. Clérot, S. Lykke Danielsen, F. Dorgeuille, A. Dupas, A. Franzen, P. Bukhave Hansen, D.K. Hunter, A. Kloch, **R. Krähenbühl**, B. Lavigne, A. Le Corre, C. Raffaelli, M. Schilling, J.-C. Simon, and L. Zucchelli

"Transparent Optical Packet Switching: The European ACTS KEOPS Project Approach"

Journal of Lightwave Technology, **16**, pp. 2117 - 2134, Dec. 1998

Y. Acremann, T. Heinzel, K. Ensslin, **E. Gini**, **H. Melchior**, and M. Holland

"Individual Scatterers as Microscopic Origin of Equilibration Between Spin-Polarized Edge Channels in the Quantum Hall Regime"

Physical Review B, **59**, pp. 2116 - 2119, Jan. 1999

D. Huber, **M. Bitter**, T. Morf, C. Bergamaschi, **H. Melchior**, and H. Jäckel

"46 GHz Bandwidth Monolithic InP/InGaAs *pin*/SHBT Photoreceiver"

Electronics Letters, **35**, pp. 40 - 41, Jan. 1999

A. Corchia, C. Antonini, A. D'Ottavi, A. Mecozzi, F. Martelli, P. Spano, **G. Guekos**, and R. Dall'Ara

"Mid-Span Spectral Inversion without Frequency Shift for Fiber Dispersion Compensation: A System Demonstration"

IEEE Photonics Technology Letters, **11**, pp. 275 - 277, Feb. 1999

T. Houbavlis, K. Zoiros, K. Vlachos, T. Papakyriakopoulos, H. Avramopoulos,

F. Girardin, **G. Guekos**, R. Dall'Ara, S. Hansmann, and H. Burkhard

"All-Optical XOR in a Semiconductor Optical Amplifier-Assisted Fiber Sagnac Gate"

IEEE Photonics Technology Letters, **11**, pp. 334 - 336, March 1999

R. Paschotta, R. Häring, **E. Gini**, **H. Melchior**, and U. Keller

"Passively Q-Switched 0.1-mJ Fiber Laser System at 1.53 μm "

Optics Letters, **24**, pp. 388 - 390, March 1999

G.J. Spühler, R. Paschotta, R. Fluck, B. Braun, M. Moser, G. Zhang, **E. Gini**, and U. Keller

"Experimentally Confirmed Design Guidelines for Passively Q-Switched Microchip Lasers using Semiconductor Saturable Absorbers"

Journal of the Optical Society of America B, **16**, pp. 376 - 388, March 1999

R. Bockstaele, Thierry Coosemans, Carl Sys, Luc Vanwassenhove, An van Hove, Bart Dhoedt, Ingrid Moerman, Peter van Daele, Roel G. Baets, **Richard Annen**, **Hans Melchior**, Jon Hall, Paul L. Heremans, Marnik Brunfaut, and Jan van Campenhout

"Realization and Characterization of 8 x 8 Resonant Cavity LED Arrays Mounted onto CMOS Drivers for POF-Based Interchip Interconnections"

IEEE Journal of Selected Topics in Quantum Electronics, **5**, pp. 224 - 235, March/April 1999

I. Zacharopoulos, I. Tomkos, D. Syvridis, F. Girardin, **L. Occhi**, and **G. Guekos**

"Influence of Phase Mismatch on a Spectral Inverter Based on Four-Wave Mixing in Dispersion-Shifted Fiber at 10 Gb/s"

IEEE Photonics Technology Letters, **11**, pp. 430 - 432, April 1999

J. Leuthold, P.-A. Besse, **E. Gamper**, **M. Dülk**, **S. Fischer**, **G. Guekos**, and **H. Melchior**

"All-Optical Mach-Zehnder Interferometer Wavelength Converters and Switches with Integrated Data- and Control-Signal Separation Scheme"

Journal of Lightwave Technology, **17**, pp. 1056 - 1066, June 1999

S. Bouchoule, R. Lefèvre, E. Legros, F. Devaux, **H. Melchior**, **M. Dülk**, **R. Hess**, E. Lach, H. Bülow, G. Veith, J.R. Burie, J.F. Cadiou, F. Brillouet, J. Hourany, D. Hoffman, B. Sartorius, K.S. Jepsen, A.T. Clausen, A. Buxens, H.N. Poulsen, K.E. Stubkjaer, H. Burkhard, and H.-J. Schöll

"Photonic Technologies for Ultra-High-Speed Information Highways: I. 40 Gbit/s TDM Components and Subsystems"

Optical Fiber Technology, **5**, Invited Paper, pp. 275 - 300, July 1999

S. Pajarola, **G. Guekos**, P. Nizzola, and H. Kawaguchi

"Dual-Polarization External-Cavity Diode Laser Transmitter for Fiber-Optic Antenna Remote Feeding"

IEEE Transactions on Microwave Theory and Techniques, **47**, pp. 1234 - 1240, July 1999

H. Soto, D. Erasme, and **G. Guekos**

"Cross-Polarization Modulation in Semiconductor Optical Amplifiers"

IEEE Photonics Technology Letters, **11**, pp. 970 - 972, Aug. 1999

T. Houbavlis, K. Zoiros, A. Hatziefremidis, H. Avramopoulos, **L. Occhi**, **G. Guekos**, S. Hansmann, H. Burkhard, and R. Dall'Ara

"10 Gbit/s All-Optical Boolean XOR with SOA Fibre Sagnac Gate"

Electronics Letters, **35**, pp. 1650 - 1652, Sept. 1999

Ch.K. Nadler, E.K. Wildermuth, M. Lanker, W. Hunziker, and H. Melchior
"Polarization Insensitive, Low-Loss, Low-Crosstalk Wavelength Multiplexer Modules"
IEEE Journal of Selected Topics in Quantum Electronics, **5**, pp. 1407 - 1412, Sept./Oct. 1999

S. Fischer, M. Dülk, M. Puleo, R. Girardi, E. Gamper, W. Vogt, W. Hunziker, E. Gini, and H. Melchior
"40-Gb/s OTDM to 4 x 10 Gb/s WDM Conversion in Monolithic InP Mach-Zehnder Interferometer Module"
IEEE Photonics Technology Letters, **11**, pp. 1262 - 1264, Oct. 1999

S. Fischer, M. Dülk, E. Gamper, W. Vogt, E. Gini, H. Melchior, W. Hunziker, D. Nettet and A.D. Ellis
"Optical 3R Regenerator for 40 Gbit/s Networks"
Electronics Letters, **35**, pp. 2047 - 2049, Nov. 1999

J. Leuthold, M. Mayer, J. Eckner, **G. Guekos, H. Melchior**, and Ch. Zellweger
"Material Gain of Bulk 1.55 μm InGaAsP/InP Semiconductor Optical Amplifiers Approximated by a Polynomial Model"
Journal of Applied Physics, **87**, pp. 618 - 620, Jan. 2000

M. Bitter, R. Bauknecht, W. Hunziker, and H. Melchior
"Monolithic InGaAs-InP p-i-n/HBT 40-Gb/s Optical Receiver Module"
IEEE Photonics Technology Letters, **12**, pp. 74 - 76, Jan. 2000

K. Hamamoto, **E. Gini, C. Holtmann, H. Melchior** and T. Sasaki
"Active Multimode Interferometer Laser Diode Demonstrated via 1.48 μm High Power Application"
Electronics Letters, **36**, pp. 138 - 139, Jan. 2000

Conference Publications (chronological)

M. Dülk, S. Fischer, E. Gamper, W. Vogt, E. Gini, H. Melchior, W. Hunziker, M. Puleo, and R. Girardi
"Full 40 Gbit/s OTDM to WDM Conversion: Simultaneous Four Channel 40:10 Gbit/s All-Optical Demultiplexing and Wavelength Conversion to Individual Wavelengths"
Postdeadline Papers Optical Fiber Communication Conference and the International Conference on Integrated Optics and Optical Fiber Communication (OFC/IOOC'99), pp. PD17-1 - 3, San Diego, California, U.S.A., Feb. 1999

L. Vanwassenhove, R. Baets, B. Dhoedt, P. Van Daele, P. Heremans, J. Van Campenhout, J. Hall, R. Michailzik, **H. Melchior**, H. Thienpont, R. Vounckx, A. Neyer, D.C. O'Brien, J. Van Koetsem, F.-T. Lentens, and D. Litaize
"Technologies for Two-Dimensional Optical Interconnect Between CMOS IC's"
Proceedings 9th European Conference on Integrated Optics and Technical Exhibition (ECIO'99), pp. 423 - 428, Torino, Italy, April 1999

M. Bitter, R. Bauknecht, W. Hunziker, and H. Melchior
"Monolithically Integrated 40-Gb/s InP/InGaAs PIN/HBT Optical Receiver Module"
Proceedings 11th International Conference on Indium Phosphide and Related Materials (IPRM'99), Davos, Switzerland, pp. 381 - 384, May 1999

D. Huber, **M. Bitter, E. Gini**, A. Neiger, T. Morf, C. Bergamaschi, and H. Jäckel
"50 GHz Monolithically Integrated InP/InGaAs PIN/HBT-Receiver"
Postdeadline Papers 11th International Conference on Indium Phosphide and Related Materials (IPRM'99), Davos, Switzerland, pp. 6 - 7, May 1999

H. Schneibel, C. Graf, R. Bauknecht, and H. Melchior
"High Current InP Double Hetero Bipolar Transistor Driver Circuit for Laser Diodes"
Proceedings 11th International Conference on Indium Phosphide and Related Materials (IPRM'99), Davos, Switzerland, pp. 455 - 457, May 1999

M. Le Pallec, R. Bauknecht, M. Bitter, and H. Melchior
"A New Concept for InP-HBT Fabrication Process"
Proceedings 11th International Conference on Indium Phosphide and Related Materials (IPRM'99), Davos, Switzerland, pp. 471 - 474, May 1999

R. Häring, R. Paschotta, **E. Gini, H. Melchior**, and U. Keller
"Sub-Nanosecond Pulses from Passively Q-Switched Microchip Lasers at 1.53 μm "
Proceedings Conference on Lasers and Electro-Optics (CLEO'99), Baltimore, U.S.A., pp. 518 - 519, May 1999

H.L. Offerhaus, D.J. Richardson, R. Paschotta, R. Häring, **E. Gini, H. Melchior**, and U. Keller
"0.1 mJ Pulses from a Passively Q-Switched Fiber Source"
Proceedings Conference on Lasers and Electro-Optics (CLEO'99), Baltimore, U.S.A., pp. 248, May 1999

K. Zoiros, T. Houbavlis, K. Vlachos, H. Avramopoulos, F. Girardin, **G. Guekos**, S. Hansmann, and H. Burkhard
"10 GHz Boolean XOR with Semiconductor Optical Amplifier Fiber Sagnac Gate"
Proceedings Conference on Lasers and Electro-Optics (CLEO'99), Baltimore, U.S.A., pp. 379 - 380, May 1999

L. Schares, Z-Y. Chen, G. Debarge, Y. Jaouen, and G-H. Duan
"Multi-Wavelength Mixing in a Semiconductor Optical Amplifier and its
Consequence in a Preamplified Wavelength Division Multiplexing System"
Proceedings Conference on Lasers and Electro-Optics (CLEO'99), Baltimore, U.S.A.,
pp. 241 - 242, May 1999

H. Soto, D. Erasme, and **G. Guekos**
"All-Optical Switch Demonstration Using a Birefringence Effect in a Semiconductor
Optical Amplifier"
Proceedings The Pacific Rim Conference on Lasers and Electro-Optics (CLEO/Pacific
Rim'99), Seoul, Korea, pp. 888 - 889, Aug./Sept. 1999

K. Hamamoto, E. Gini, Ch. Holtmann, **H. Melchior**, and T. Sasaki
"Area Size Dependency of Active Multi-Mode-Interferometer Laser Diode"
Extended Abstracts No. 3, The 60th Autumn Meeting of The Japan Society of Applied
Physics, Kobe, Japan, p. 982, Sept. 1999

E. Gini, E. Gamper, W. Vogt, and H. Melchior
"Monolithic Integration of Passive Waveguides with Active SOA's and Phase Shifters
for $\lambda = 1.55 \mu\text{m}$ Using Four Step LP-MOVPE Growth"
Proceedings 25th European Conference on Optical Communication (ECOC'99), Nice,
France, pp. I-174 - I-175, Sept. 1999

T. Houbavlis, K. Zoiros, A. Hatziefremidis, H. Avramopoulos, **L. Occhi**, G. Guekos,
S. Hansmann, and H. Burkhard
"10 Gbit/s Boolean XOR with Semiconductor Optical Amplifier Fiber Sagnac Gate"
Proceedings 25th European Conference on Optical Communication (ECOC'99), Nice,
France, pp. 252 - 253, Sept. 1999

M. Brunfaut, J. Depreitere, W. Meeus, J.M. van Campenhout, **H. Melchior, R. Annen,**
P. Zenklusen, R. Bockstaele, L. Vanwassenhove, J. Hall, A. Neyer, B. Wittmans,
J. van Koetsem, R. King, H. Thienpont, and R. Baets
"A Multi-FPGA Demonstrator with POF-based Optical Area Interconnect"
Proceedings Laser and Electro-Optics 1999 Annual Meeting, San Francisco, U.S.A.,
pp. 625 - 626, Nov. 1999

M. Brunfaut, J. Depreitere, W. Meeus, J.M. van Campenhout, **H. Melchior, R. Annen,**
P. Zenklusen, R. Baets, L. Vanwassenhove, J. Hall, B. Wittman, P. Heremans, R. King,
H. Thienpont, and J. van Koetsem
"The OIIC Optoelectronic FPGA Demonstrator"
Laser and Electro-Optics 1999 Annual Meeting, San Francisco, U.S.A., pp. 625 - 626,
Nov. 1999

Oral Presentations 1999

J.P. Hall, R. Baets, **R. Annen**, P. Zenklusen, K.J. Ebeling, A. Neyer, B. Wittmann, V. Baukens, H. Thienpont
"Components for 1 Gbit/s/channel, 2-D Array Optically Interconnected CMOS for the OIIC 'Gigalink' Demonstrator"
MEL-ARI OPTO 3rd Annual Workshop, Athens, Greece, Oct. 13 - 15, 1999

M. Bitter, R. Bauknecht, W. Hunziker, and H. Melchior
"Monolithically Integrated 40-Gb/s InP/InGaAs PIN/HBT Optical Receiver Module"
11th International Conference on Indium Phosphide and Related Materials (IPRM'99), Davos, Switzerland, May 16 - 20, 1999

D. Huber, **M. Bitter**, **E. Gini**, A. Neiger, T. Morf, C. Bergamaschi, and H. Jäckel
"50 GHz Monolithically Integrated InP/InGaAs PIN/HBT-Receiver"
11th International Conference on Indium Phosphide and Related Materials (IPRM'99), Davos, Switzerland, May 16 - 20, 1999

M. Dülk, **St. Fischer**, E. Gamper, W. Vogt, E. Gini, H. Melchior, W. Hunziker, M. Puleo, and R. Girardi
"Full 40 Gbit/s OTDM to WDM Conversion: Simultaneous Four Channel 40:10 Gbit/s All-Optical Demultiplexing and Wavelength Conversion to Individual Wavelengths"
Optical Fiber Communication Conference and the International Conference on Integrated Optics and Optical Fiber Communication (OFC/IOOC'99), San Diego, California, U.S.A., Feb. 21 - 26, 1999

E. Gini, E. Gamper, W. Vogt, and H. Melchior
"Monolithic Integration of Passive Waveguides with Active SOA's and Phase Shifters for $\lambda = 1.55 \mu\text{m}$ Using Four Step LP-MOVPE Growth"
25th European Conference on Optical Communication (ECOC'99), Nice, France, Sept. 26 - 30, 1999

K. Zoiros, T. Houbavlis, K. Vlachos, H. Avramopoulos, F. Girardin, **G. Guekos**, S. Hansmann, and H. Burkhard
"10 GHz Boolean XOR with Semiconductor Optical Amplifier Fiber Sagnac Gate"
Conference on Lasers and Electro-Optics (CLEO'99), Baltimore, U.S.A., May 23 - 28, 1999

H. Soto, D. Erasme, and **G. Guekos**
"All-Optical Switch Demonstration Using a Birefringence Effect in a Semiconductor Optical Amplifier"
The Pacific Rim Conference on Lasers and Electro-Optics (CLEO/Pacific Rim'99), Seoul, Korea, Aug. 30 - Sept. 3, 1999

M. Lanker

"Design and Realisation of InP and Silica Based Optical Planar Lightwave Circuits"
Presentation at TU Delft, Faculty ITS, Delft, the Netherlands, Nov. 26, 1999

H. Melchior

"Mach-Zehnder Interferometer Based Semiconductor Optical Amplifiers Devices for Ultrahigh Speed Applications"
Semiconductor Optical Amplifier Meeting, Swiss Federal Institute for Technology Lausanne, Switzerland, March 19, 1999

L. Vanwassenhove, R. Baets, B. Dhoedt, P. Van Daele, P. Heremans, J. Van Campenhout, J. Hall, R. Michailzik, **H. Melchior**, H. Thienpont, R. Vounckx, A. Neyer, D.C. O'Brien, J. Van Koetsem, F.-T. Lentens, and D. Litaize
"Technologies for Two-Dimensional Optical Interconnect Between CMOS IC's"
9th European Conference on Integrated Optics and Technical Exhibition (ECIO'99), Torino, Italy, April 13- 16, 1999

R. Häring, R. Paschotta, **E. Gini**, **H. Melchior**, and U. Keller
"Sub-Nanosecond Pulses from Passively Q-Switched Microchip Lasers at 1.53 μm "
Conference on Lasers and Electro-Optics (CLEO'99), Baltimore, U.S.A., May 23 - 28, 1999

H.L. Offerhaus, D.J. Richardson, R. Paschotta, R. Häring, **E. Gini**, **H. Melchior**, and U. Keller
"0.1 mJ Pulses from a Passively Q-Switched fiber source"
Conference on Lasers and Electro-Optics (CLEO'99), Baltimore, U.S.A., May 23 - 28, 1999

M. Puleo, R. Girardi, M. Scofet, R. Hess, M. Dülk, S. Fischer, **H. Melchior**, S. Bouchoule, E. Legros, A. Ramdane
"Dimostrazione di un'interfaccia OTDM-WDM tutto-ottica, basata su dispositivi fotonici in InP, con capacità di 40 Gbit/s"
Fotonica 99, 6 Convegno Nazionale sulle Tecniche Fotoniche nelle Telecomunicazioni, Trento, Italy, June 2 - 4, 1999

H. Melchior

"Photonic Integrated Circuits using Semiconductor Optical Amplifiers"
Optical Amplifiers and Their Applications (OAA'99), Nara, Japan, June 9 - 11, 1999

H. Melchior

"Advances in Integrated Photonics"
Plenary Presentation, Micro Optics Conference (MOC'99), Makuhari Messe, Chiba, Japan, July 14 - 16, 1999

H. Melchior

"Optoelectronics in the Swiss Federal Institute of Technology Zurich"
Presentation at the NTT Photonic Laboratories, Ibaraki, Japan, July 19, 1999

H. Melchior

"Passive Alignment Packaging of Semiconductor Lasers and OEIC's"
Tutorial at Conference on Lasers and Electro-Optics, CLEO/Pacific Rim 99, Seoul, Korea, Aug. 30 - Sept. 3, 1999

K. Hamamoto, E. Gini, Ch. Holtmann, **H. Melchior**, and T. Sasaki

"Area Size Dependency of Active Multi-Mode-Interferometer Laser Diode"
The 60th Autumn Meeting of The Japan Society of Applied Physics, Kobe, Japan, Sept. 1 - 4, 1999

H. Melchior

"Indium Phosphide Waveguide Switch-Modules for Optically Controlled Optical Signal Processing at 40 and 80 Gbit/s"
Invited Paper, Institute of Electronics, Information and Communication Engineers-Meeting, Tokyo, Japan, Sept. 7 - 10, 1999

H. Melchior

"Semiconductor Optical Amplifiers for High-Speed All-Optical Signal Processing"
Presentation at the Swiss Society for Optics and Microscopy / Priority Program Optics II Meeting, Neuchâtel, Switzerland, Sept. 15 - 17, 1999

H. Melchior

"From Indium Phosphide Waveguide Switches to All-Optical High Speed Signal Processing Components"
Invited presentation at Semiconductor Components for Optical Signal Processing Symposium, Danish Technical University, Lyngby, Denmark, Oct. 4, 1999

M. Brunfaut, J. Depreitere, W. Meeus, J.M. van Campenhout, **H. Melchior**, R. Annen, P. Zenklusen, R. Bockstaele, L. Vanwassenhove, J. Hall, A. Neyer, B. Wittmans, J. van Koetsem, R. King, H. Thienpont, and R. Baets

"A Multi-FPGA Demonstrator with POF-based Optical Area Interconnect"
Proceedings Laser and Electro-Optics 1999 Annual Meeting, San Francisco, U.S.A., Nov. 7 - 11, 1999

M. Brunfaut, J. Depreitere, W. Meeus, J.M. van Campenhout, **H. Melchior**, R. Annen, P. Zenklusen, R. Baets, L. Vanwassenhove, J. Hall, B. Wittman, P. Heremans, R. King, H. Thienpont, and J. van Koetsem

"The OIIC Optoelectronic FPGA Demonstrator"
Laser and Electro-Optics 1999 Annual Meeting, San Francisco, U.S.A., Nov. 7 - 11, 1999

L. Occhi, L. Schares, R. Gutiérrez-Castrejón, M. Dülk, S. Fischer, and G. Guekos
"Chirp Induced by XGM and FWM in Bulk Semiconductor Optical Amplifiers used
for Wavelength Conversion"
COST Action 267, 1st Workshop on "Semiconductor Devices for Optical Signal
Processing", Rome, Italy, April 22, 1999

T. Houbavlis, K. Zoiros, A. Hatziefremidis, H. Avramopoulos, **L. Occhi**, **G. Guekos**,
S. Hansmann, and H. Burkhard
"10 Gbit/s Boolean XOR with Semiconductor Optical Amplifier Fiber Sagnac Gate"
25th European Conference on Optical Communication (ECOC'99), Nice, France,
Sept. 26 - 30, 1999

L. Schares, Z-Y. Chen, G. Debarge, Y. Jaouen, and G-H. Duan
"Multi-Wavelength Mixing in a Semiconductor Optical Amplifier and its
Consequence in a Preamplified Wavelength Division Multiplexing System"
Conference on Lasers and Electro-Optics (CLEO'99), Baltimore, U.S.A., May 23 - 28,
1999

L. Schares, R. Gutiérrez-Castrejón, L. Occhi, G. Guekos, K. Zoiros, K. Vlachos, and
H. Avramopoulos
"High Repetition Rate, Wavelength Tunable Fiber Ring Laser based on Optical
Modulation of a Semiconductor Optical Amplifier"
European Semiconductor Laser Workshop 1999, Paris, France, Sept. 24 - 25, 1999

Thin Film Physics Group

Press Releases

M. Krejci and A.N. Tiwari

"Solarzellen zum Aufkleben und Rollen: Leichte und flexible Dünnschicht-Solarzellen als Folien"

Neue Zürcher Zeitung, Forschung und Technik, p. 74, Nov. 3, 1999

A.N. Tiwari, and H. Zogg

"Dünne Halbleiterschichten auf flexibler Folie für billigeren Sonnenstrom: Weltrekord mit flexiblen Solarzellen"

Bild des Monats, Swiss National Science Foundation, Dec. 20, 1999

http://www.snf.ch/WWW_e/News_e/PM201299_d.html

A.N. Tiwari, and H. Zogg

"Zürcher Solarzellen zum Rollen"

Tages-Anzeiger, Wissen im Bild, Dec. 22, 1999

Book Chapters

G. Springholz, Z. Shi, and **H. Zogg**

"Molecular Beam Epitaxy of Narrow Gap IV-VI Semiconductors"

Heteroepitaxy: Thin Film Systems, Edited by W.K. Liu and M.B. Santos, Chapter 14, pp. 621 - 688, World Scientific Publishing, Singapore, ISBN 981-02-3390-6, 1999

Journal Publications (chronological)

V. Nadenau, H.W. Schock, **M. Krejci, F.-J. Haug, A.N. Tiwari, and H. Zogg**

"Microstructure of Cu-rich CuGaSe₂ Thin Films"

Diffusion-and-Defect-Data-Part-B (Solid-State-Phenomena), **67-68**, pp. 397 - 401, 1999

V. Nadenau, D. Hariskos, H.-W. Schock, **M. Krejci, F.-J. Haug, A.N. Tiwari, H. Zogg**, and G. Kostorz

"Microstructural Study of CdS/CuGaSe₂ Interfacial Region in CuGaSe₂ Thin Film Solar Cells"

Journal of Applied Physics, **85**, pp. 534 - 542, Jan. 1, 1999

J. John, and H. Zogg

"Infrared p-n-Junction Diodes in Epitaxial Narrow Gap PbTe Layers on Si Substrates"

Journal of Applied Physics, **85**, pp. 3364 - 3366, March 15, 1999

S. Schön, **H. Zogg**, and U. Keller
"Growth of Novel Broadband High Reflection Mirrors by Molecular Beam Epitaxy"
Journal of Crystal Growth, **201-202**, pp. 1020 - 1023, May 1999

A.N. Tiwari, M. Krejci, F.-J. Haug, H. Zogg, V. Zelezny, and V. Vorlicek
"Heteroepitaxy of CuIn_xSe_y : Material for High Efficiency and Stable Thin Film Solar Cells"
Journal of Crystal Growth, **201**, pp. 1057 - 1060, May 1999

F.-J. Haug, M. Krejci, A.N. Tiwari, and H. Zogg
"Solar-Energy - Technologically Advanced - Economically Profitable - Ecologically Compatible"
Bi-monthly Review of the Swiss-Japanese Chamber of Commerce, Swiss-Japanese Journal, pp. 28 - 32, Sept. 1999

A.N. Tiwari, M. Krejci, F.-J. Haug, and H. Zogg
"12.8% Efficiency $\text{Cu}(\text{In,Ga})_x\text{Se}_y$ Solar Cell on a Flexible Polymer Sheet"
Progress in Photovoltaics: Research and Applications, **7**, pp. 393 - 397, Sept./Oct. 1999

Conference Publications (chronological)

H. Zogg, C. Paglino, J. John, P. Müller, and K. Alchalabi
"Photovoltaic Lead-Chalcogenide on Silicon Infrared Focal Plane Arrays"
Invited paper, Atti della Fondazione Giorgio Ronchi, Anno, 1998, pp. 65 - 67:
Proceedings IVth Int. Workshop on Advanced Infrared Technology and Applications,
Florence, Italy

H. Zogg
"Epitaxial Lead-Chalcogenide on Silicon Layers for Thermal Imaging Applications"
Invited paper, Proceedings 4th Int. Conference on Material Science and Material
Properties for Infrared Optoelectronics (SPIE 3890), Kiev, Ukraine, pp. 22 - 26, 1998

H. Zogg
"Photovoltaic IV-VI on Silicon Infrared Devices for Thermal Imaging Applications"
Invited Paper, Proceedings SPIE 3629 Photonics West, San Jose, CA, U.S.A.,
pp. 52 - 62, Jan. 1999

A.N. Tiwari, M. Krejci, F.-J. Haug, and H. Zogg
" $\text{Cu}(\text{In,Ga})_x\text{Se}_y$ Epitaxial Layers and Polycrystalline Solar Cells"
Invited paper, Proceedings 10th Int. Workshop on Physics of Semiconductor Devices
(IWPSD), Delhi, India, pp. 1227 - 1234, Dec. 1999

H. Zogg, K. Alchalabi, and A.N. Tiwari

"Photovoltaic IV-VI on Silicon Infrared Devices for Thermal Imaging"

Invited paper, Proceedings 10th Int. Workshop on Physics of Semiconductor Devices (IWPSD), Delhi, India, pp. 51 - 56, Dec. 1999

Oral Presentations

K. Alchalabi, and H. Zogg

"Epitaxial Growth of PbSe/PbTe on BaF₂ (100) and PbTe (100) and Possible Quantum Dots by Dislocation Superlattices"

SPG-Tagung, Berne, Switzerland, Feb. 25 - 26, 1999

D. Bätzner, A. Romeo, H. Zogg, and A.N. Tiwari

"Study of the Back Contacts on CdTe/CdS Solar Cells"

SPG-Tagung, Berne, Switzerland, Feb. 25 - 26, 1999

D. Bätzner, A. Romeo, H. Zogg, and A.N. Tiwari

"A Study of the Back Contacts on CdTe/CdS Solar Cells"

European Material Research Society 1999 Spring Meeting, Strasbourg, France, June 1 - 4, 1999

F.-J. Haug, M. Krejci, H. Zogg, and A.N. Tiwari

"Characterization of CuGa_xSe_y/ZnO for Superstrate Solar Cells"

European Material Research Society 1999 Spring Meeting, Strasbourg, France, June 1 - 4, 1999

F.-J. Haug, M. Krejci, H. Zogg, and A.N. Tiwari

"Cu(In,Ga)Se₂ Superstrate Solar Cells on Transparent Conducting Zinc Oxide Layers"

11th International Photovoltaic Science and Engineering Conference, Sapporo, Japan, Sept. 20 - 24, 1999

M. Krejci, V. Nadenau, D. Hariskos, A.N. Tiwari, F.-J. Haug, H. Zogg,

H.-W. Schock

"Microstructural Study of the CdS/CuGaSe₂ Interface in Thin Film Solar Cell"

SPG-Tagung, Berne, Switzerland, Feb. 25 - 26, 1999

M. Krejci, F.-J. Haug, H. Zogg, A.N. Tiwari, V. Nadenau, and H. Schock

"Characterization of Microstructural Defects and Inclusions in CdS/CuGaSe₂"

European Material Research Society 1999 Spring Meeting, Strasbourg, France, June 1 - 4, 1999

A. Romeo, D. Bätzner, M. Wagner, J.R. Günther, H. Zogg, and A.N. Tiwari

"High Efficiency CdTe/CdS Solar Cells by a Recrystallization Process"

SPG-Tagung, Berne, Switzerland, Feb. 25 - 26, 1999

A. Romeo, D. Bätzner, H. Zogg, and A.N. Tiwari

"Recrystallization in CdTe/CdS"

European Material Research Society 1999 Spring Meeting, Strasbourg, France,
June 1 - 4, 1999

A. Romeo, D. Bätzner, H. Zogg, and A.N. Tiwari

"Influence of CdS Growth Process on the Structural and Photovoltaic Properties of CdTe/CdS Solar Cells"

11th International Photovoltaic Science and Engineering Conference, Sapporo, Japan,
Sept. 20 - 24, 1999

A.N. Tiwari, F.-J. Haug, M. Krejci, and H. Zogg

"Heteroepitaxy of CuIn_xSe_y : A Review of the Material and Interface Properties"

Invited Presentation at the European Material Research Society 1999 Spring Meeting,
Strasbourg, France, June 1 - 4, 1999

A.N. Tiwari, M. Krejci, F.-J. Haug, and H. Zogg

"Development of $\text{Cu}(\text{In,Ga})\text{Se}_2$ Solar Cells on Polymer with a Record Efficiency of 12.8%"

Invited Presentation at the 11th International Photovoltaic Science and Engineering
Conference, Sapporo, Japan, Sept. 20 - 24, 1999

A.N. Tiwari, M. Krejci, F.-J. Haug, and H. Zogg

" $\text{Cu}(\text{In,Ga})\text{Se}_2$ Epitaxial Layers and Polycrystalline Solar Cells"

Invited Presentation at the 10th International Workshop on The Physics of Semiconductor
Devices (IWSPD), New Delhi, India, Dec. 14 - 18, 1999

H. Zogg

"Photovoltaic IV-VI on Silicon Infrared Devices for Thermal Imaging Applications"

"Photodetectors: Materials and Devices IV"

Invited Presentation SPIE Optoelectronics 1999 International Symposium, San Jose,
U.S.A., Jan. 23 - 29, 1999

H. Zogg, Q. Lai, and K. Alchalabi

"Bleichalkogenid IR-Sensoren auf Silizium: Maximale Empfindlichkeiten und 2-d
Array auf aktivem Si-Substrat"

29. IR-Kolloquium, Freiburg i. Brg., April 27, 1999

H. Zogg

"Growth on Device Applications of Epitaxial Narrow Gap Lead Chalcogenide Layers
on Silicon Substrates"

Invited Presentation Solid State Seminar, University of Oslo, Norway, Aug. 23, 1999

H. Zogg, K. Alchalabi, and D. Gössi

"Epitaxial IV-VI-on-Si Layers: Dislocation Density Reduction Mechanisms and Dependence on Sensor Device Properties"

The 9th International Conference on Narrow Gap Semiconductors, **ng9**, Berlin, Germany, Sept. 26 - Oct. 1, 1999

H. Zogg, K. Alchalabi, and A.N. Tiwari

"Photovoltaic IV-VI on Silicon Infrared Devices for Thermal Imaging Applications"

Invited Presentation at the 10th International Workshop on The Physics of Semiconductor Devices (IWSPD), New Delhi, India, Dec. 14 - 18, 1999

Ph.D. and Diploma Theses
of the IQE
1999

PH.D. THESES IN PHYSICS 1999

Krejci, Martin

"Preparation and Characterization of Heteroepitaxial CuIn_xSe_y Layers and Cu(In,Ga)Se_2 Substrate Solar Cells"

ETH Zurich, No. 13142 (Prof. Dr.G. Kostorz, PD Dr. H. Zogg, Dr. A.N. Tiwari & Dr. R. Heinrich)

DIPLOMA THESES IN PHYSICS 1999

Marcoz, Olivier

"Technology and Characterization of GaN Ohmic Contacts, Schottky Diodes and Electroluminescent Diodes"

ETH Lausanne/Zurich, March 1999 (Prof. Dr. M. Illegems, Prof. Dr. H. Melchior)

Gössi, Dominik B.

"Herstellung und Charakterisierung heteroepitaktischer Bleichalkogenid-Strukturen"

ETH Zurich, Oct. 1999 (Prof. Dr. H. Melchior, PD Dr. H. Zogg)

Rapp, Martin

"Growth and Characterization of Polycrystalline Cu(In,Ga)S_2 Thin Film Solar Cells"

ETH Zurich, Oct. 1999 (Prof. Dr. H. Melchior, PD Dr. H. Zogg)